Subsonic Aircraft Wing Conceptual Design Synthesis and Analysis

Abderrahmane Badis[*]

Electrical and Electronic Communication Engineer from UMBB (Ex.INELEC), Independent Electronics, Aeronautics, Propulsion, Well Logging and Software Design Research Engineer, Takerboust, Aghbalou, Bouira 10007, Algeria

Email: Badis.dahmane@gmail.com

Abstract

This paper exposes a simplified preliminary conceptual integrated method to design an aircraft wing in subsonic speeds up to Mach 0.85. The proposed approach is integrated, as it allows an early estimation of main aircraft aerodynamic features, namely the maximum lift-to-drag ratio and the total parasitic drag. First, the influence of the Lift and Load scatterings on the overall performance characteristics of the wing are discussed. It is established that the optimization is achieved by designing a wing geometry that yields elliptical lift and load distributions. Second, the reference trapezoidal wing is considered the base line geometry used to outline the wing shape layout. As such, the main geometrical parameters and governing relations for a trapezoidal wing are reviewed in details. Third, the integrated design method is introduced through an evocative flowchart that describes the wing design process, whose objectives are essentially the determination and the optimization of the different wing parameters, essentially: Wing Area, Sweep Angle, Aspect Ratio, Taper Ratio, Thickness and Twist. Furthermore, refined and assessed formulas identified from an exhaustive literature study and historical trends yielding accurate and logical estimation of each parameter described in the optimization flowchart are provided. Finally, the capability of the proposed method is investigated through two design examples for jet and propeller aircrafts. The obtained layouts are tested and verified through simulations using the NASA OpenVSP simulation software.

Keywords: Aircraft Wing; Subsonic Flight; Conceptual Design; Elliptical Distributions; OpenVSP.

----

* Corresponding author.

1. Introduction

The wing is considered as the most important part of an aircraft. Its primary function is the generation of the required aerodynamic lift force needed to sustain the aircraft weight in the air. Although the lift force is the main product of the wing, the drag force and the pitching moment are two undesirable products that must be minimized. Despite the fact that other aircraft's components contribute in the total lift, the wing remains the main lift generating surface, thus the design of the wing play a major role in the aircraft overall aerodynamics. The aircraft wing must be designed to meet the requirements of the different fight phases mainly takeoff, cruise and landing. Aircrafts spend most of the time in cruise flight. It is therefore important to design the wing to operate efficiently in this segment. Wing Lift and Load distributions determine the wing performance characteristics such as induced drag, structural weight and stalling features. The wing geometry shapes its lift and load distributions, as such the wing design process objectives are essentially the determination and the optimization of the different wing parameters, mainly: Wing Area, Sweep Angle, Aspect Ratio, Taper Ratio, Thickness and Twist. Figure 1 illustrates the spreading of the lift coefficient along the wing span, this is referred to as the lift distribution. This distribution is very important in aerodynamics calculations. On the other hand, Figure 2 illustrates the span-wise variation of lift coefficient times the local sectional chord, this is referred to as the load distribution. The primary application of the load distribution is in controllability analysis and wing structural design.
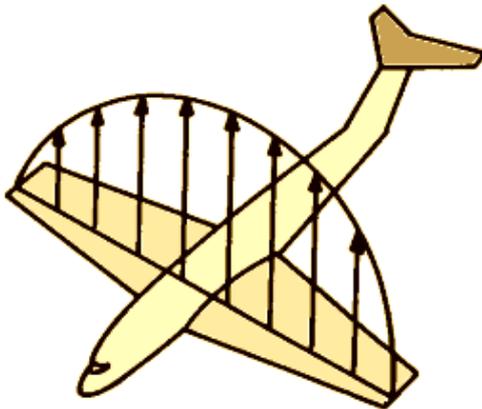

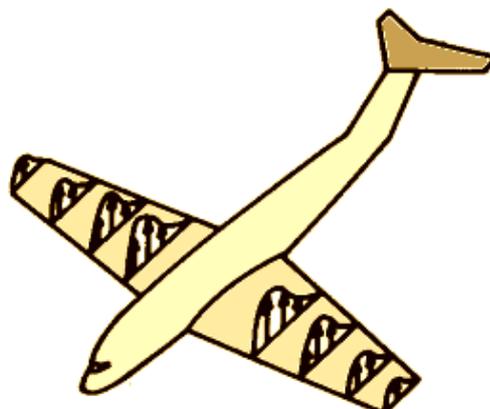**Figure 1:** Wing Lift Distribution   **Figure 2:** Wing Load Distribution

It turns out that for subsonic flights, the elliptical distributions result in the least induced drag and pitching moment while yielding the best stall characteristics for a given wing span and total lift, as such the design objectives are to get both lift distribution and load distribution to be elliptical.

This paper proposes a simplified approach for a preliminary conceptual design of an aircraft wing in the subsonic range while considering the above scheme requirements. The method and materials are valid for speeds reaching Mach 0.85. In addition to the wing characterization, the proposed technique allows the estimation of the primary factors characterizing the overall aircraft aerodynamic and physical features such as lift-to-drag ratio at cruise and loiter conditions, zero-lift drag coefficient or parasitic drag, the total aircraft

wetted area and the takeoff weight.

Even though the sizing of the aircraft is not part of the paper scope, it is worth mentioning that the wing geometry and its features are influencing all other aircraft components, as such the consolidation of all the results obtained could easily be used in the dimensioning of the aircraft components such as Vertical Tail, Horizontal tail, Fuselage, Landing Gear etc.

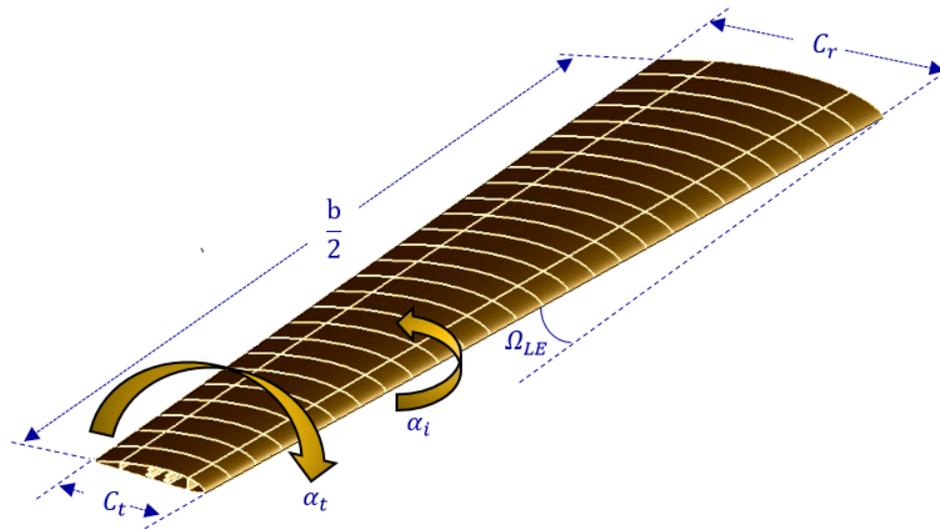## 2. Wing Geometry Description

Figure 3: Geometric Properties of Trapezoidal Wings

The aircraft wing shape could be outlined in several ways. The reference trapezoidal wing is the base line geometry used to begin the wing layout. Figure 3 illustrates the most important angles and parameters used to describe it. While the wing area, often denoted by (S), constitutes the back bone of the wing as it depends on lift requirements during the different flight phases. The standard meaning of (b) is wing span, it denotes the distance from wing tip to wing tip. The symbol (C) is used for the chord length of an airfoil at any point along the wing span. Therefore, the subjects named (C_r) and (C_t) are the chord length at the wing root and the wing tip respectively. The symbol (Ω) is used for wing sweep angle with the subscript (LE) denoting the wing leading edge. Furthermore, (α_t) refers to the angle of twist; geometric twist is achieved by twisting the wing so that the tip airfoil is at a lower angle of attack than the root airfoil. On the other hand, aerodynamic twist is achieved by changing the airfoil camber so that the tip airfoil has less camber than the root airfoil. The wing incidence (α_i) is the angle between fuselage center line and the wing chord line at root, it is often referred to as the wing setting angle.

Based on the above, further wing characterizing parameters are defined as follow:

Aspect ratio,

$$A = \frac{b^2}{S} \qquad (1)$$

If the aspect ratio and the wing area are known, Equation (1) could be solved for the wing span.

$$b = \sqrt{A\,S} \qquad (2)$$

Taper Ratio,

$$\lambda = \frac{c_t}{c_r} \qquad (3)$$

Where,

$$C_{root} = \frac{2S}{[b(1+\lambda)]} \qquad (4)$$

The aspect ratio and the Taper Ratio are two main parameters which affect aerodynamic characteristics of the wing. They are used by the designer to change the planform of the wing.

The aspect ratio is the primary ruling factor of the wing lift-to-drag ratio. Increasing the aspect ratio will decrease the wing drag and vice versa. On the other hand, the increase in aspect ratio will cause an increase in the wing span, this will overload the wing structure. It is clear that the selection of the aspect ratio compromises between the lift to drag ratio and the wing structural weight, a pertinent value must be selected to obtain the best results for these two conflicting imports.

The second parameters influencing the lift-to-drag ratio is the wing taper ratio. Tapering the wing will decrease the drag and increase the lift. In addition, a considerable wing weight saving is gained.

Despite the fact that the aspect and taper ratios are the primary influencing actors in drag reduction, the increase in speed is drastically increasing the air drag, it can be compared to an invisible spring compressing the front of the aircraft's wings, as speed is close to the speed of sound the air becomes as solid as a wall [1]. To overcome this drag force, it is common to sweep the leading edge behind the Mach cone. The sweep of the quarter chord line ($\Omega_{1/4}$) is the sweep most related to subsonic flight [2]. The leading edge sweep (Ω_{LE}) is the angle of concern in supersonic flight. Equation (5) allows converting from one sweep angle to another.

$$\tan \Omega_{1/4} = \tan \Omega_{LE} - \frac{1}{A}\frac{(1-\lambda)}{(1+\lambda)} \qquad (5)$$

While the wing span characterizes the lateral extent of the aerodynamic forces acting on the wing, the mean aerodynamic chord ($\bar{C}$) characterizes the axial extent of these forces. The mean aerodynamic chord is usually approximated by the mean geometric chord [3], it could be computed using Equation (6).

$$\bar{C} = \frac{2\left(1+\lambda+\lambda^2\right)}{3(1+\lambda)} C_r \qquad (6)$$

The mean chord distance $\overline{Y}$ from the wing root chord is computed using Equation (7).

$$\overline{Y} = \left(\frac{b}{6}\right)\left(\frac{1+2\lambda}{1+\lambda}\right) \tag{7}$$

In subsonic flow, the entire wing has its mean aerodynamic center approximately at 25 % of the mean aerodynamic chord. The mean aerodynamic chord and the aerodynamic center are used to position the wing properly. Also, the mean aerodynamic chord is very important in the stabilization computations [3].

3. Wing Conceptual Integrated Method Design

The design process is diagrammed in Figure 4, it is an Integrated Method based on an iterative process that considers the most important aerodynamic elements of the aircraft. It combines the historical trend of some parameters with the aerodynamic theory to come up with a refined sizing of the wing along with an estimation of the aircraft aerodynamic features to meet the design requirements.
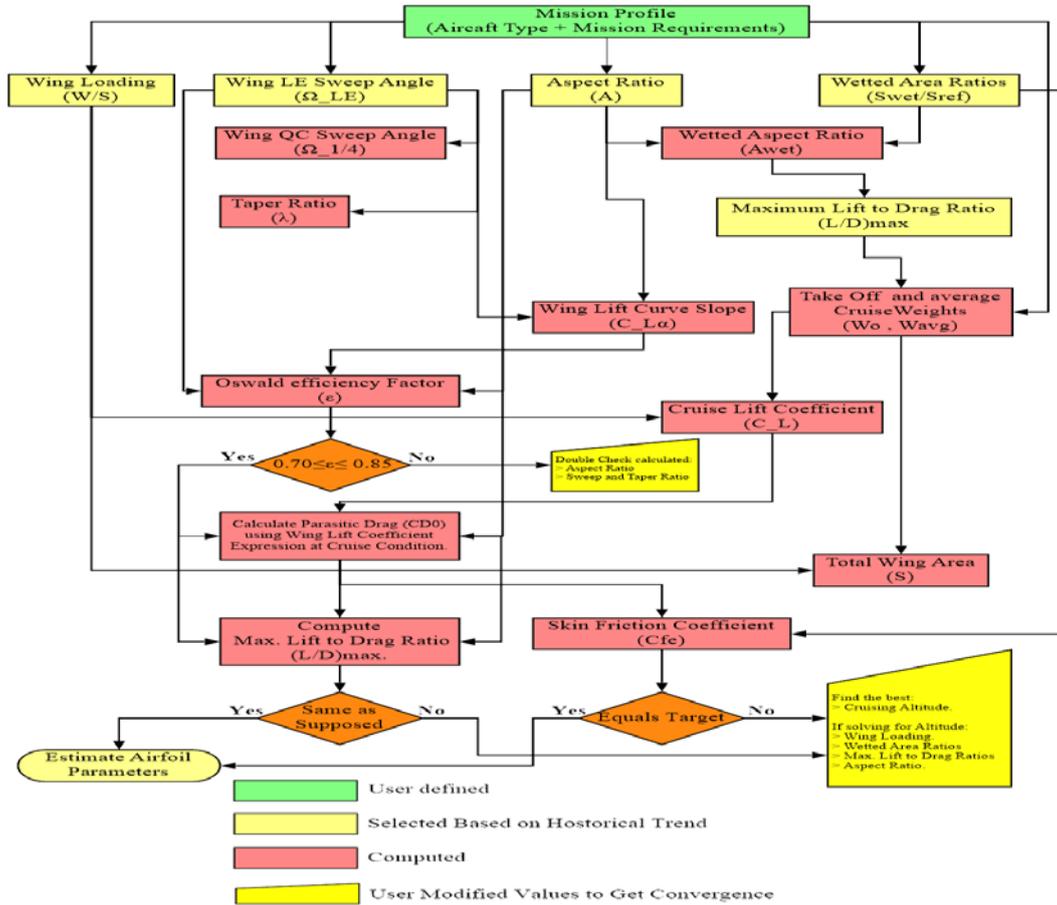

Figure 4: Integrated Wing Design Method

Although some factors in the diagram have not been described yet to the reader and without getting into details at this stage, it is clear that the dependencies among these parameters are plenty, a simple variation of any of the factors will influence the whole set. The Wing Design Integrated Method illustrated uses the data and

information provided in the mission profile to compute values for Aspect Ratio, Wetted Area Ratios, Maximum Lift-to-Drag Ratio, Wing Loading and the Leading Edge Sweep Angle based on their historical trends. After that a list of parameters are computed including Wing Lift Curve Slope, The Taper Ratio, the Quarter Chord Sweep Angle, the Takeoff Weight and the Average Weight in the Cruise Segment, the Reference Wing Area, the Oswald Efficiency Factor, the Lift Coefficient at Cruise and the Zero-lift Drag Coefficient. The parasitic drag is calculated using the wing lift coefficient at cruise condition. This latter is used to calculate the maximum lift-to-drag ratio. Convergence is achieved when the postulated and calculated ratios equal. The Equivalent Skin Friction Coefficient is the main quality control parameter used to validate the results, this is done through direct comparison with historical values for some commonly known aircrafts. The proposed design could be solved either for the proposed wing aerodynamic features at cruise through calculation of the cruise altitude or define the aerodynamic features of the wing for a given altitude. Once the outcomes are validated, some important airfoil features are estimated namely the Relative Thickness, the Ideal Lift Coefficient and the maximum Lift Coefficient, etc.

4. Wing Parameters Design Equations

In this section, a mathematical model is proposed for each parameters; aerodynamic theory, empirical formulas selected from an exhaustive literature study and appropriate interpolation techniques of historical data are the baselines used to provide best estimate expressions.

4.1. Takeoff Wing Loading Estimation

The wing loading is one of the most essential parameters that plays an important role in the performance of the airplane. It is defined as the total weight of the aircraft divided by the reference wing. In general the wing loading often refers to the takeoff wing loading. To ensure that the wing is providing enough lift in all circumstances, an optimal value must be estimated. The airplanes flying at high subsonic speed need high wing loading from the consideration of cruise. As such, complicated high lift devices are employed to reduce take-off and landing distances [4]. Enhanced representative values for Takeoff Wing Loading as provided by [2] are summarized in Table 1. These data constitute a good starting values for the design optimization process.

Table 1: Typical Takeoff Wing Loading

Aircraft Class	Typical Takeoff Wing Loading (Kg/m^2)
Sailplane	29
Homebuilt	54
General aviation – single engine	83
General aviation – twin engine	127
Twin turboprop	195
Jet trainer	244
Jet fighter	342
Jet transport / bomber	586
Super transporter / bomber	816

To ease the use of the data provided in Table 1, a plot of the takeoff wing loading versus aircraft categories is generated as illustrated in Figure 5. To explore the chart efficiently, some commonly known aircraft 'wing loadings have been presented on the graph.
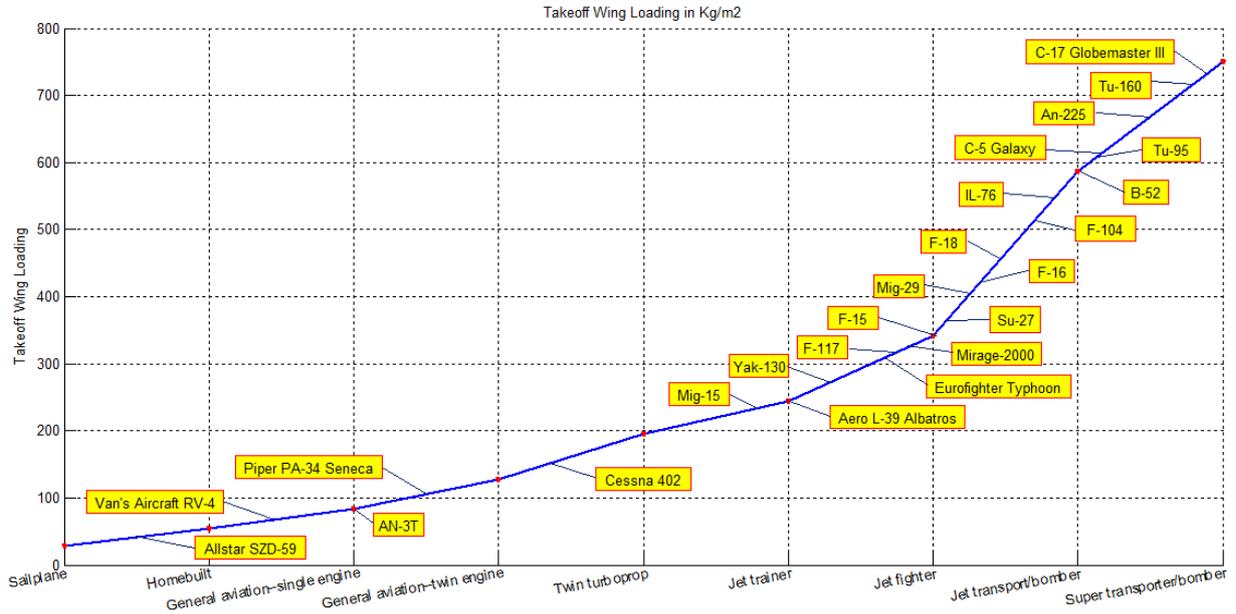

Figure 5: Takeoff Wing Loading Selection Chart

Equation (8) is an exponential interpolation formula that best fit the curve displayed in Figure 5. We define (Φ) as a Loading Index varying from 0 for Sailplanes to 8 for Super-transporter or Heavy Bombers.

$$\left(\frac{W}{S}\right)_{TO} = (34.66) \operatorname{Exp}\left(\frac{4}{10}.\Phi\right) \qquad (8)$$

Where,

$$0 \leq \Phi \leq 8$$

4.2. Aspect Ratio

The Aspect ratio is defined as the ratio between the wing span and the main aerodynamic chord line. Equation (1) which is usually used in all calculations, defines it as the square of the wingspan divided by the wing area. As such, a long and narrow wing is characterized with high aspect ratio and vice versa.

The Aspect Ratio is recognized as being a key player in wing aerodynamic behavior; a wing with high aspect ratio will perform well at slow speeds and produce large quantities of lift allowing sustained and long endurance flights, but at the expense of maneuverability and airspeed [5]. On the other hand, a wing with a low aspect ratio has either a short span such as fighters or a thick chord such as Space Shuttles, this will allow the aircraft to fly faster while offering a swift maneuverability.

Some aircraft such as F-14, Mig-27, F-111, Tu-160 and the B-1 are equipped with variable geometry wings, thus mutable aspect ratio to take advantages of both configurations at low and high speeds.

Table 2 summarizes typical values and equations for Equivalent Aspect Ratios as provided by [2]. The equivalent aspect ratio uses an equivalent wing area that includes canard areas in defining the aspect ratio. Practically, the canard presents about 10 % to 20 % of the total lifting area, as such the actual aspect ratio would be the estimated equivalent one divided by 0.9 to 0.75.

Table 2: Typical Equivalent Aspect Ratio

Aircraft Class	Equivalent Aspect Ratio	
Sailplane	4.464	
Propeller Aircraft		
Homebuilt	6.0	
General aviation – single engine	7.6	
General aviation – twin engine	7.8	
Agricultural aircraft	7.5	
Twin turboprop	9.2	
Flying Boat	8.0	
Jet Aircraft		
Equivalent $A = aM_{max}^C$	a	C
Jet trainer	4.737	-0.979
Jet fighter – dog fighter	5.416	-0.622
Jet fighter – Other	4.110	-0.622
Military Cargo / bomber	5.570	-1.075
Jet Transport	7.500 to 10.0	0

4.3. *Wing Leading Edge Sweep Angle*

The angle between the wing leading edge and the y-axis of the aircraft is called leading edge sweep. The sweep of the wing is used to improve the wing aerodynamic features mainly the lift, drag and pitching moment by delaying the compressibility effects.

In subsonic flights, the quarter chord sweep $(\Omega_{1/4})$ angle must be selected accurately as the subsonic lift due angle of attack acts at the quarter chord. As per Equation (5), for a fixed aspect ratio, the taper ratio, the quarter chord and leading edge angles are thoroughly interrelated.

It was found that for aircrafts speeds less than Mach 0.3 the compressibility effect is negligible, thus no sweep angle is recommended for the wing, as its drawbacks dominates the improvements it yields. For example, by

using 5 degrees of sweep angle, the aircraft drag could be reduced by 2 percent, but the cost of manufacturing is increase by 15 percent and the manufacturing complexity is bigger. As such a straight wing would be preferred [6]. In practice, for subsonic airplanes, a sweep angle of 35 degrees is rarely exceeded. It is also noticeable that theoretically there is no difference between sweeping a wing aft and sweeping it forward [2]. Despite the high maneuverability gained, only experimental aircrafts were built with forward-swept wings such as the X-29 and Su-47, this is mainly limited by the cost and weight penalty associated with the stiffness required and the associated inherent divergent pitch behavior.

Figure 6 shows a historical trend line for wing leading edge sweep versus Mach number [2]. For initial wing layout the trend line is very reasonable and provides satisfactory design values.
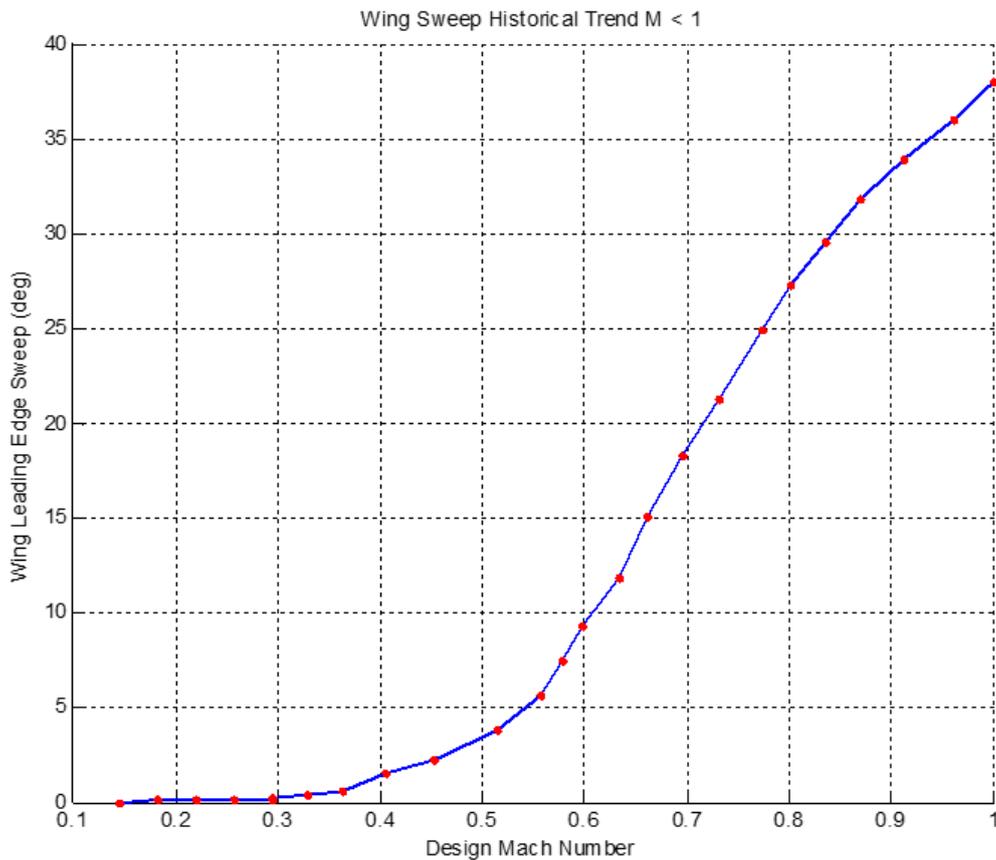

Figure 6: Wing Sweep Historical Trend for Subsonic Speeds

Equation (9) is a polynomial interpolation formula that best fit the curve displayed in Figure 6. We define (M) as the maximum aircraft Mach number.

$$\Omega_{LE} = (-484.49).M^4 + (971.41).M^3 - (574.01).M^2 + (131,66).M - 9.87 \qquad (9)$$

Where,

$$0.3 \leq M \leq 0.85$$

4.4. Taper Ratio and Quarter Chord Sweep

As started in the introduction, the induced drag occurs when the lift distribution is elliptical. Figure 6 illustrates the results of NACA wind tunnel to determine the taper ratio required to approximate an elliptical lift distribution for a swept untwisted wing [2] for a given quarter chord sweep angle.

Taper ratios much lower than 0.2 should be avoided for all wings with the exception of delta wings; very low taper ratio tends to stimulate tip stall. Low swept wings have generally taper ratios of about 0.4 to 0.5 and most swept wings have a taper ratios of about 0.2 to 0.3.
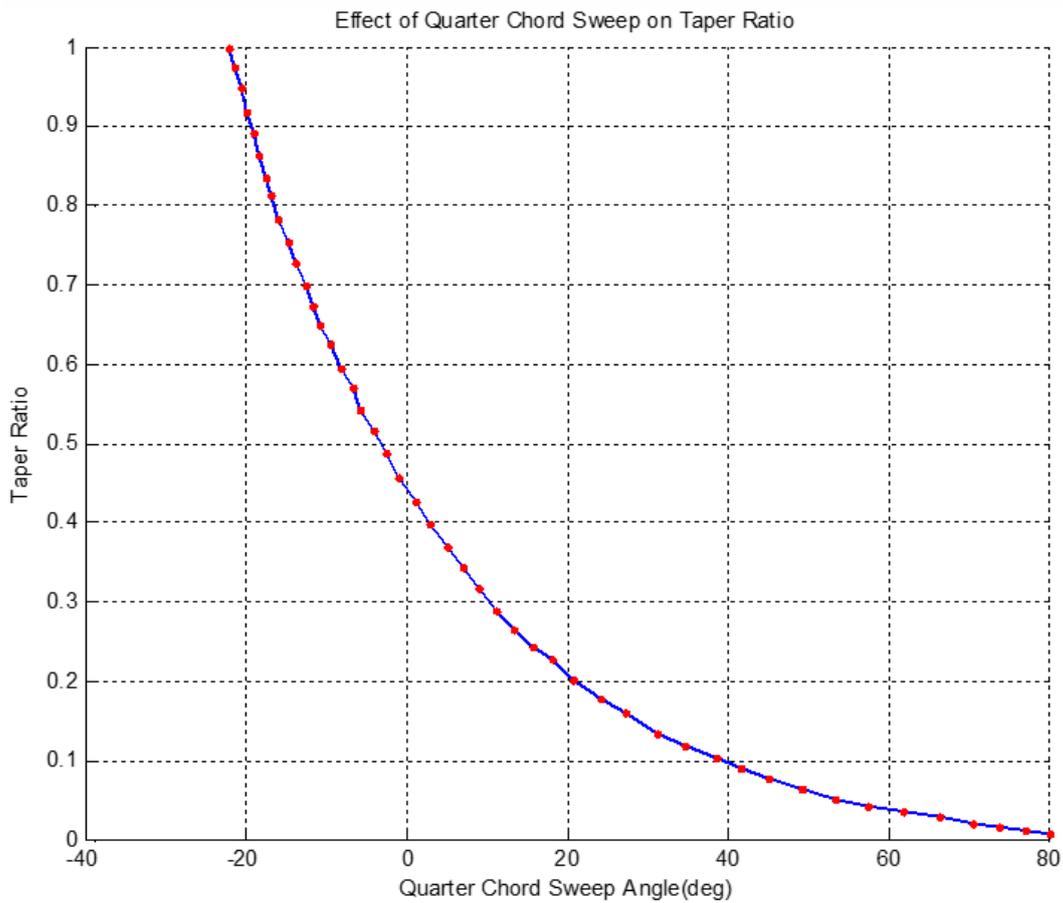

Figure 7: Taper Ratio - Quarter Chord Sweep Trend line for an Elliptical Lift Distribution

Equation (10) is a polynomial interpolation formula that best fit the curve displayed in Figure 7. We define $(\Omega_{1/4})$ as the wing quarter chord sweep angle

$$\lambda = (-2 \times 10^{-10}).\Omega_{1/4}^{5} + (4 \times 10^{-8}).\Omega_{1/4}^{4} - (4 \times 10^{-6}).\Omega_{1/4}^{3} + (3 \times 10^{-4}).\Omega_{1/4}^{2} - (16 \times 10^{-3}).\Omega_{1/4} + 0.4409$$

(10)

Where,

$$-22 \ \leq \Omega_{1/_4} \leq 80$$

Equation (10) alone won`t serve to compute the Taper Ratio, it is important to consider both Equations (5) and (9). The methodology to solve for the three dependent variables ; Taper Ratio, Leading Edge and Quarter Chord Sweep angles would be as follow:

a. Compute the leading edge sweep angle using Equation (9).

b. Inject a value for the quarter chord sweep angle in Equation (10) to compute the taper ratio.

c. Compute the leading edge sweep angle using Equation (5).

d. If the values computed in steps (a) and (c) are equal then go ahead with these values for the three parameters, otherwise repeat steps (b) and (c) till convergence is achieved.

Note: It is recommended to use an Excel Table to deal with the iterative computations described above.

4.5. Aircraft Takeoff Weight Buildup

The total weight of an aircraft at the start of the mission for which it was designed is called the Design Takeoff Gross Weight. The Design Takeoff Gross Weight is summation of crew weight, payload weight, fuel weight and the empty weight as described by Equation (11).

$$W_0 = W_{crew} + W_{payload} + W_{fuel} + W_{empty} \tag{11}$$

Rearranging Equation (11) yields Equation (12),

$$W_0 = \frac{W_{crew} + W_{payload}}{1 - \left(\frac{W_f}{W_0}\right) - \left(\frac{W_e}{W_0}\right)} \tag{12}$$

Equation (12) states that W_0 could be determined if the fraction of Fuel Weight to Design Takeoff Gross Weight (W_f/W_0) and Empty Weight to Design Takeoff Gross weight (W_e/W_0) are estimated.

4.5.1. Empty-Weight Fraction Estimation

The empty-weight fraction is estimated statistically from historical data as shown in Table 3 [2]. A curve-fit equation is developed to best estimate the empty-weight fraction. Each type of aircraft is characterized by its corresponding coefficients.

In general, the empty-weight fraction varies from 0.3 to 0.7, it reduces as the total weight of the aircraft is increasing.

Note that if the aircraft got a variable-sweep the estimated empty-weight fraction is multiplied by 1.04. If composite materials are used then the empty-weight fraction is reduced by some 05 %. Moreover, for composite fiberglass-epoxy homebuilt aircrafts the empty-weight fraction must be decreased by 25 %.

Table 3: Empty-Weight Fraction Estimation

Aircraft Class	Coefficients	
$\left(\dfrac{W_e}{W_0}\right) = A.W_0^C.K_{vs}$	**A**	**C**
Sailplane - Unpowered	0.86	-0.05
Sailplane - Powered	0.91	-0.05
Homebuilt – Metal / Wood	1.19	-0.09
Homebuilt – Composite	0.99	-0.09
General aviation – single engine	2.36	-0.18
General aviation – twin engine	1.51	-0.10
Agricultural aircraft	0.74	-0.03
Twin turboprop	0.96	-0.05
Flying Boat	1.09	-0.05
Jet Trainer	1.59	-0.10
Jet Fighter	2.34	-0.13
Military Cargo / bomber	0.93	-0.07
Jet Transport	1.02	-0.06
K_{vs} is the variable sweep constant: ▪ K_{vs} = 1.04 if variable sweep ▪ K_{vs} = 1.00 if fixed sweep		

4.5.2. *Fuel-Weight Fraction Estimation*

Computing the fuel fraction requires considering the mission profiles. The amount of mission fuel is dependent upon the mission to be accomplished, the aerodynamics of the aircraft and the specific fuel consumption of the engine. For safety reasons, it is required to add some fuel reserves for extra loiter and/or cruise time of typically 20 to 30 minutes. Moreover, it is important to account for the trapped fuel which could not be pumped out of the tanks. Once the fuel fraction is estimated, an additional 06 % is added to count for the reserve and trapped fuel.

Figure 8 illustrate a typical mission profile. To ease the analysis, the different mission segments are considered individually. The segments are sequentially numbered from (0) for the mission start through (5) for landing, where (1) is usually the warmup and takeoff, (2) Climb, (3) Cruise and (4) for Loiter.

The aircraft weight at the end of every segment are also number in similar manner; W_0 is the takeoff gross weight, W_1 is the weight after warm-up and takeoff, W_2 is the weight after the Climb, W_3 would be the weight after cruise, W_4 after loiter. Finally, W_5 is the weight of the aircraft at the end of the mission. For any mission segment, the mission segment fraction is expressed are the ratio between the weight at the beginning and at the

end of the segment. The ratio of the aircraft weight at the end W_N (N Segments) to the initial weight W_0 is calculated by multiplying the weight fractions.

The warm-up, climb and landing weight-fractions could be estimated relying on historical data as summarized in Table 4 [2].
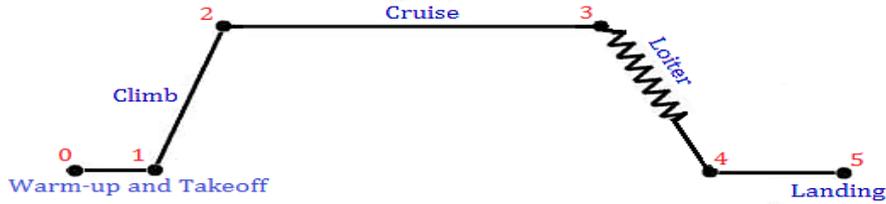

Figure 8: Typical Mission Profile

Table 4: Warm-up, Climb and Landing Historical Weight-Fractions

Mission Segment	Weight Fraction $\left(\dfrac{W_i}{W_{i-1}}\right)$
Warm-up and Takeoff	0.970
Climb	0.985
Landing	0.995

Equation (13) is used to calculate the cruise segment weight-fraction, it is obtained based on the Breguet range equation.

$$\frac{W_i}{W_{i-1}} = \text{Exp}\left(\frac{-RC}{V_c \left(\frac{L}{D}\right)_{cruise}}\right) \tag{13}$$

Where,

- ❖ R: Range in meters (m).
- ❖ C: Jet-Engine Specific Fuel Consumption in $1/_s$
- ❖ V_c: Velocity in $m/_s$
- ❖ $\left(\frac{L}{D}\right)_{cruise}$: Lift-to-Drug ratio at cruise

Equation (14) is used to calculate the loiter segment weight-fraction, it is derived from on the endurance equation.

$$\frac{W_i}{W_{i-1}} = Exp\left(\frac{-EC}{\left(\frac{L}{D}\right)_{loiter}}\right) \tag{14}$$

Where,

- ❖ E: Endurance time in Seconds (s)
- ❖ C: Jet-Engine Specific Fuel Consumption in $1/s$
- ❖ $\left(\frac{L}{D}\right)_{Loiter}$: Lift-to-Drug ratio at loiter

For jet engines, Specific Fuel Consumption (C) is defined as the rate of engine fuel consumption divided by the resulting thrust. For propeller engine, the specific Fuel Consumption is given as Brake Specific Fuel Consumption (C_{bhp}) or brake horsepower, which is the rate of fuel consumption divided by the power produced at some propeller efficiency (η_p).

Equations (13) and (14) are both using the Jet-Engine Specific Fuel Consumption, as such if a propeller engine is used, then an equivalent Jet-Engine Specific Fuel Consumption is calculated using Equation (15).

$$C = C_{bhp}\frac{V}{(167.7)\eta_P} \tag{15}$$

Where,

- ❖ V: Velocity in meters/seconds (m/s).
- ❖ η_p: Propeller Efficiency.

Table 5 provides typical jet-engines Specific Fuel Consumption (C), while Table 6 provides typical values for Propeller Specific Fuel Consumption (C_{bhp}) and Propeller Efficiency (η_p).

Table 5: Typical Jet-Engine Specific Fuel Consumption (C)

Engine Type	Cruise	Loiter
Pure Turbojet	0.9	0.8
Low-bypass Turbofan	0.8	0.7
High-bypass Turbofan	0.5	0.4

Table 6: Typical Propeller Specific Fuel Consumption (C_{bhp}) and Propeller Efficiency (η_p)

Engine Type	Cruise	Loiter
Piston-prop (fixed pitch)	0.4 / 0.8	0.5 / 0.7
Piston-prop (variable pitch)	0.4 / 0.8	0.5 / 0.8
Turboprop	0.5 / 0.8	0.6 / 0.8

It is important to use consistent units in Equations (14) and (15), the choice made on the Specific Fuel Consumption is mainly to get reciprocal seconds. If other units are provided then one could use the conversion Equations (16) and (17) for (C) and (C_{bhp}) respectively.

$$\text{Conversion for C: } \left[\frac{lb}{lbf/h}\right] = \left[\frac{1}{h}\right] = 28.257 \left[\frac{g}{KN/s}\right] \tag{16}$$

$$\text{Conversion for } C_{bhp}: \left[\frac{lb}{hp/h}\right] = 608.277 \left[\frac{g}{Kw/h}\right] \tag{17}$$

Converting reciprocal hours to reciprocal seconds use the Equation (18).

$$\left[\frac{1}{s}\right] = \frac{\left[\frac{1}{h}\right]}{3600} \tag{18}$$

Typical Conversion Example:

The Kuznetsov NK-32 is a low-bypass turbofan engine, it is the largest and most powerful engine ever fitted on a combat aircraft [7]. Four NK-32's are powering the Russian strategic bomber Tupolev Tu-160. This engine produces 245 KN of thrust in maximum afterburner. At subsonic flight, its specific fuel consumption is 20.68 $\frac{g}{KN.s}$. Using conversion Equation (16), C = 0.732 $\frac{1}{h}$ and using (18), C= $2.033 \times 10^{-4} \frac{1}{s}$.

Total fuel fraction is then computed using Equation (19), where a value of 06 % extra fuel is assumed for reserves and trapped fuel.

$$\frac{W_f}{W_0} = 1.06 \left(1 - \frac{W_N}{W_0}\right) \tag{19}$$

Where,

$$\frac{W_N}{W_0} = \frac{W_1}{W_2} \times \frac{W_3}{W_2} \times \frac{W_4}{W_3} \times \frac{W_5}{W_4} \times \frac{W_6}{W_5} \times \dots \times \frac{W_i}{W_{i-1}} \tag{20}$$

Equation (12) could now be solved iteratively by guessing the takeoff gross weight, calculating the statistical empty-weight fraction and then calculating the takeoff gross weight. This process is repeated for few iterations till conversion is achieved.

The only remaining unknowns in both Equations (13) and (14) are the Lift-to-Drag ratios at Cruise and Loiter, which are a metric of the aircraft aerodynamic efficiency, this will be examined in the next section.

4.5.3. *Lift-to-Drag Ratios Estimation*

The lift-to-drag ratio is the total amount of lift generated by the aircraft divided by the total drag created when moving through the air. A higher lift-to-drag ratio represents the foremost goal in aircraft design. It is highly dependent on the design features of the aircraft. At subsonic speeds, the lift-to-drag ratio is mostly affected by

the wing span and the wetted area. The wetted area is described as the total exposed aircraft surface that would get wet if it was dripped into water. The drag at subsonic speeds is mainly composed of two parts. The first being the induced drag, which is mainly caused by the generation of lift and it is wing span dependent. The second one is the zero-lift or parasitic drag which is mainly caused by skin-friction thus wetted-area dependent. The parasitic drag is best described when the configuration layout of the aircraft is considered (tailed versus tailless aircraft for example), the parameter used in this aspect is the wetted-area ratio. Figure 9 illustrates a spectrum of design approaches and the resulting wetted-area ratios [2].
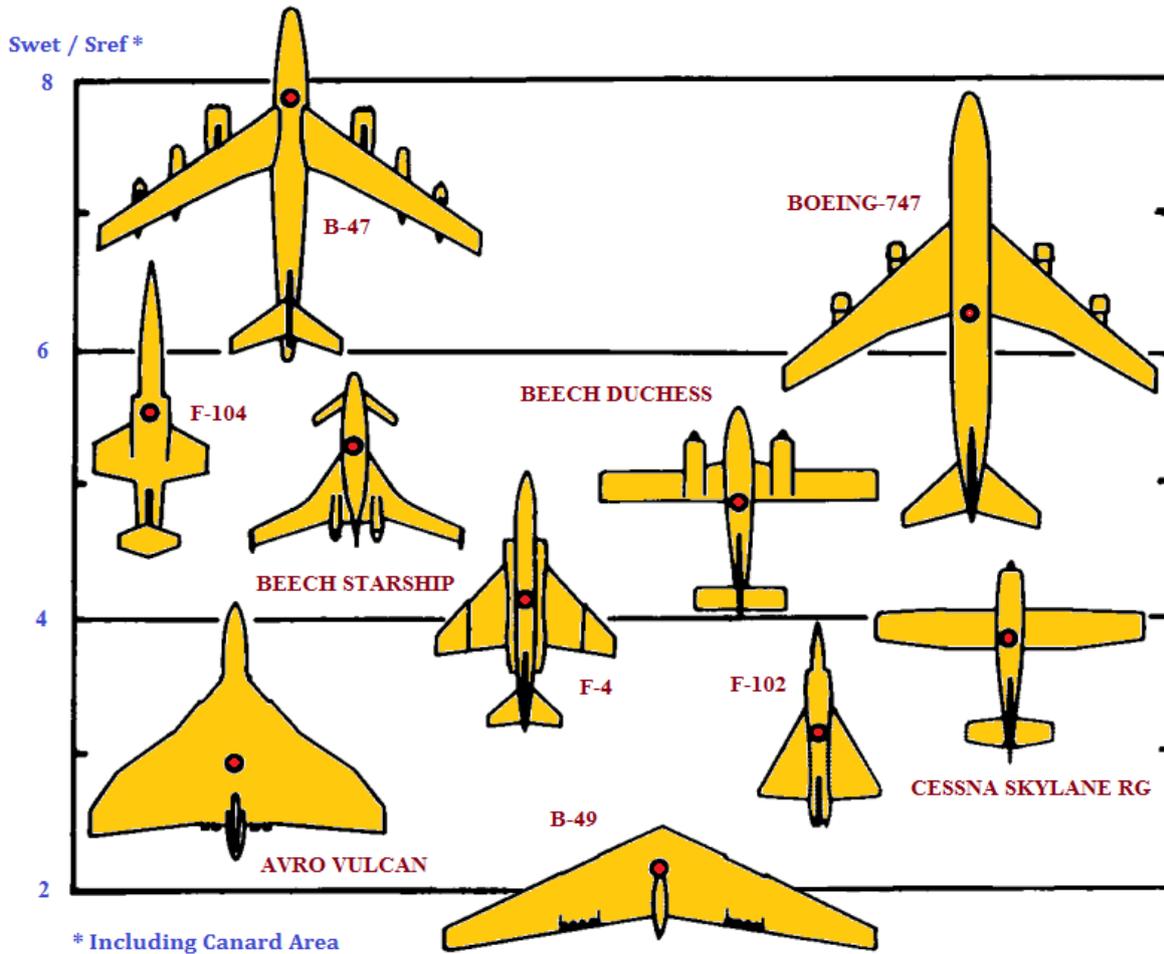
Figure 9: Design Spectrums versus Wetted Area Ratios

It is defined as a ratio between the total wetted-area divided by the wing reference area with canards included. A more reliable early estimate of the lift-to-drag ratio would be achieved if the wetted-area is used along with the aspect ratio. This suggests a new parameters, the Wetted Aspect Ratio, which is defined as the wing span squared divided by the total aircraft wetted area.

The wetted-area could be eyeball-estimated from Figure 9, then the wetted aspect ratio is calculated using Equation (21).

$$A_{wetted} = \frac{b^2}{S_{wet}} = \frac{A}{\left(S_{wet}/S_{ref}\right)} \qquad\qquad (21)$$

Once the wetted aspect ratio is calculated using Equation (21), Figure 10 [2] could then be used to estimate the maximum lift-to-drag ratio.
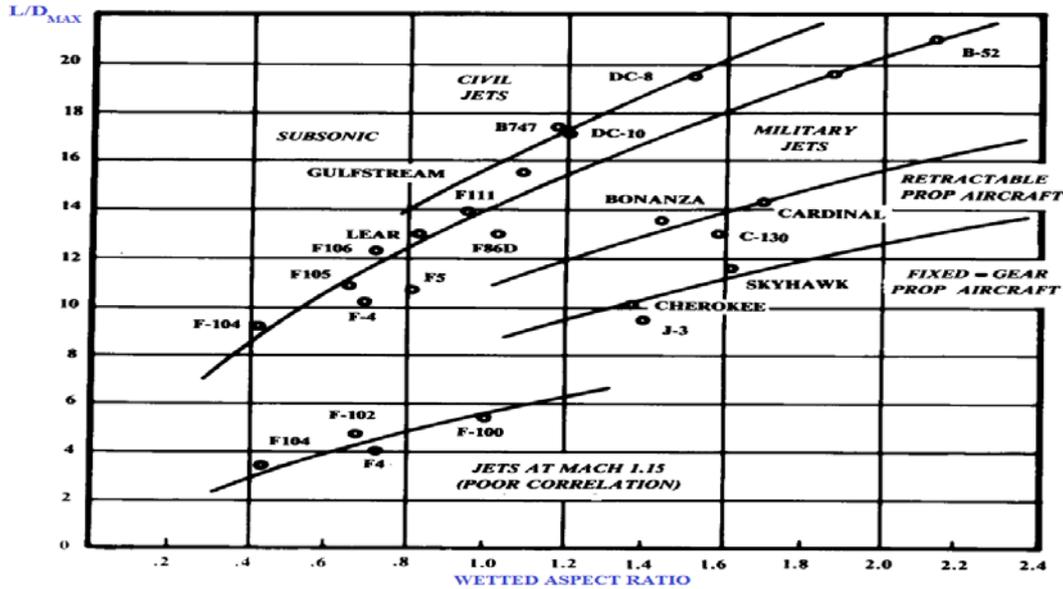

Figure 10: Maximum Lift-to-Drag Ratio Trends

As drag varies with altitude and velocity, it is important to mention that for any altitude there is a velocity which maximizes the lift-to-drag ratio. All required governing and descriptive equations are provided in the next sections.

As summarized in Table 7; the most efficient loiter for a jet aircraft occurs precisely at the velocity yielding the maximum lift-to-drag ratio. On the other hand, the most efficient loiter for a propeller aircraft occurs at a slower velocity that yield a lift-to-drag ratio of 86.6 % of the maximum lift-to-drag ratio.

Similarly, the most efficient cruise velocity for a propeller aircraft occurs at the velocity yielding the maximum lift-to-drag ratio, while the most efficient cruise for a jet aircraft occurs at slightly higher velocity yielding a lift-to-drag ratio of 86.6 % of the maximum lift-to-drag ratio.

Table 7: Cruise and Loiter Lift-to-Drag Ratios

Aircraft Powerplant	Cruise	Loiter
Jet	$0.866\left(\frac{L}{D}\right)_{max}$	$\left(\frac{L}{D}\right)_{max}$
Propeller	$\left(\frac{L}{D}\right)_{max}$	$0.866\left(\frac{L}{D}\right)_{max}$

4.6. Total Wing Area

The takeoff gross weight and the takeoff wing loading have been estimated in the previous sections. Now the total wing area could be easily calculated using Equation (22).

$$S = \frac{W_0}{\left(\frac{W}{S}\right)_{TO}} \tag{22}$$

4.7. Parasitic Drag and Equivalent Skin-Friction Coefficient

The parasitic drag (C_{D_0}) could be estimated using the Skin-Friction Method. This method is based on the fact that in subsonic cruise, a well-designed aircraft will have a parasitic drag that is mostly due to skin-friction and a small separation pressure drag which is fairly a consistent percentage of the skin-friction drag for the different classes of aircrafts. The Equivalent Skin-Friction Coefficient (C_{f_e}) is the factor that combines both skin-friction and separation drag.

The parasitic drag could be estimated by multiplying the skin-friction coefficient with the aircraft's wetted area ratio. Equation (23) and Table (8) [2] are very important in our approach for the subsonic analysis and will be used to compute the Skin-Friction Coefficient which represents a primary convergence criteria.

$$C_{D_0} = C_{fe} \frac{S_{wet}}{S_{ref}} \tag{23}$$

Table 8: Typical Equivalent Skin-Friction Coefficients

Aircraft Class	Equivalent Skin-Friction Coefficient
Bomber and civil transport	0.0030
Military cargo (high upsweep fuselage)	0.0035
Airforce fighter	0.0035
Navy fighter	0.0040
Clean supersonic cruise aircraft	0.0025
Light aircraft – single engine	0.0055
Light aircraft – twin engine	0.0045
Propeller seaplane	0.0065
Jet seaplane	0.0040

4.8. Wing Lift Slope

Equation (24) is a modified expression based on Prandtl-Glauert approximation introduced by [8] to compute the wing lift curve slope (per radian), the equation does not consider the fuselage contribution, but it is accurate enough for the initial sizing for subsonic speeds. The fuselage lift factor, endplates and winglets effects could be considered when refining the design. Note that the wing sweep tends to reduce the wing lift slope.

$$C_{L\alpha} = \frac{2\pi A}{2+\sqrt{A^2(1+\tan^2 \Omega_{LE}-M^2)+4}} \tag{24}$$

4.9. Oswald Efficiency Factor

Oswald efficiency Factor (ε) is a measure of drag due to lift efficiency also called Span Efficiency Factor. It is a measure of how elliptical is the wing lift distribution. When the Oswald span efficiency factor is closer to one, it indicates that the lift distribution is getting elliptical. In practice, the typical values for the Oswald efficiency factor wing flaps retracted are typically between 0.7 and 0.85. Although several estimation methods have been developed, Equation (25) suggested by [9] which is based on statistical data, provides a more realistic estimation of the Oswald efficiency factor. Note that the Oswald efficiency number decreases substantially with speed.

$$\varepsilon = \frac{1}{(1+0.12 \cdot M^6)\left(1+\frac{0.42+f(\lambda)\cdot A \cdot \left(10 \cdot \left(\frac{t}{c}\right)\right)^{0.33}}{\cos^2 \Omega_{1/4}}+\frac{0.1 \cdot (3N_e+1)}{(4+A)^{0.8}}\right)} \tag{25}$$

Where,

- ❖ N_e: Number of engines located over the top surface of the wing.
- ❖ $f(\lambda) = 0.005[1 + 1.5(\lambda - 0.6)^2]$: Taper ratio function.

Oswald efficiency factor is frequently linked to the drag-due-to-lift factor (K) defined in equation (26). In classical wing theory, the drag-due-to-lift factor for a wing with an elliptical lift distribution equals to one divided by the product of aspect ratio and Pi (π). However, few wings truly have an elliptical lift distribution, thus the extra drag due to the nonelliptical lift distribution and the flow separation is accounted through using the Oswald efficiency factor.

$$K = \frac{1}{\pi A \varepsilon} \tag{26}$$

4.10. Cruise and Loiter Aerodynamic Conditions

In this section, the cruise and loiter conditions potted in Table 7 are further expended. Equations for lift-to-drag ratio, lift coefficient and drag coefficient for both cruise and loiter conditions are summarized. Cruise is often defined as the aerodynamic condition that allows the aircraft a maximum flight range, while Loiter is the aerodynamic condition that allows the aircraft a maximum flight endurance. For more details on endurance and cruise flights please refer to [10].

4.10.1. Jet Cruise Equations

$$\left(\frac{L}{D}\right)_{cruise} = 0.866 \left(\frac{L}{D}\right)_{max} = \sqrt{\frac{3\pi A \varepsilon}{16 C_{D_0}}} \tag{27}$$

$$C_L = \sqrt{\frac{C_{D_0}\pi A \varepsilon}{3}} \tag{28}$$

$$C_D = \frac{4}{3} C_{D0} \tag{29}$$

4.10.2. Jet Loiter Equations

$$\left(\frac{L}{D}\right)_{Loiter} = \left(\frac{L}{D}\right)_{max} = \sqrt{\frac{\pi A \varepsilon}{4 C_{D_0}}} \tag{30}$$

$$C_L = \sqrt{\pi A \varepsilon C_{D0}} \tag{31}$$

$$C_D = 2 C_{D0} \tag{32}$$

4.10.3. Propeller Cruise Equations

$$\left(\frac{L}{D}\right)_{cruise} = \left(\frac{L}{D}\right)_{max} = \sqrt{\frac{\pi A \varepsilon}{4 C_{D_0}}} \tag{33}$$

$$C_L = \sqrt{C_{D0} \pi A \varepsilon} \tag{34}$$

$$C_D = 2 C_{D0} \tag{35}$$

4.10.4. Propeller Loiter Equations

$$\left(\frac{L}{D}\right)_{Loiter} = 0.866 \left(\frac{L}{D}\right)_{max} = \sqrt{\frac{3 \pi A \varepsilon}{16 C_{D_0}}} \tag{36}$$

$$C_L = \sqrt{3 \pi A \varepsilon C_{D0}} \tag{37}$$

$$C_D = 4 C_{D0} \tag{38}$$

4.11. Airfoil Selection
4.11.1. Airfoil Parameters Overview

In the wing design process, the airfoil selection is the second most important wing parameter to define after wing planform. The selection of the adequate airfoil for the wing is primary dictated by the flight requirements. For instance, the airfoil needed for subsonic, transonic and supersonic flight would have different design requirements. Reliability, Structural integrity, Manufacturability and cost are also important requirements to consider when selecting an airfoil. The design of the airfoil is not an easy process, a lot of expertise and advanced wind tunnel tests are necessary. Only large aircraft manufacturer have the financial means, test facilities and human resources to develop airfoils for each new aircraft designed. On the other hand, small companies or homebuilders select the needed airfoil from the free available database shared in data books or websites [11]. Before moving forward, it is important to review the main airfoils parameters. Figure 11 and 12 illustrate the two most important airfoil characterizing graphs: the variation of the lift coefficient versus the angle of attack and the variation of the drag coefficient versus lift coefficient. All associated parameters are

displayed on the figures. Table 9, provides a description for each parameter along with a typical values for each.
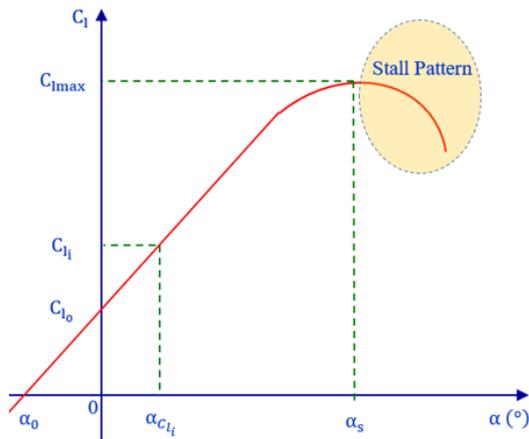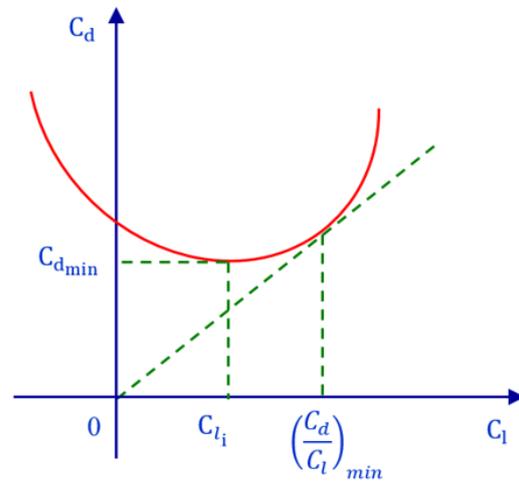

Figure 11: Lift Coefficient versus Angle of Attack   **Figure 12:** Drag Polar Plot

Table 9: Airfoils Main Parameters

Airfoil Parameter	Brief Description	Typical Values
$C_{l_{max}}$	Maximum lift coefficient: maximum capacity of an airfoil to produce non-dimensional lift.	Varies
α_s	Stall angle: angle of attack at which the airfoil stalls.	It varies from 12 to 16 degrees
C_{l_i}	Ideal lift coefficient also called Optimum Lift coefficient: lift coefficient at which the drag coefficient does not vary significantly with the minor variations of angle of attack, it usually corresponds to the minimum drag coefficient. Best to choose the cruise lift coefficient as close as possible to the ideal lift coefficient.	For subsonic aircraft, it varies from 0.1 to 0.4.
$\alpha_{C_{l_i}}$	Ideal lift coefficient angle of attack, it is very important for wing setting angle.	It varies from 2 to 5 degrees
C_{l_0}	Lift coefficient at zero angle of attack.	Varies
α_0	Zero angle of attack: angle of attack at which the lift coefficient is zero.	Around -2 degrees
C_{l_α}	Lift curve slop.	Typical value is around 2π per radian or 0.1 per degree.
Stall Pattern	It is the shape of the lift curve at and beyond the stall angle of attack. It is recommended to have an airfoil with a gentle drop in lift after the stall rather than a sharp and fast lift loss.	N/A
$C_{d_{min}}$	Minimum drag coefficient, it is the drag coefficient corresponding to the Ideal lift coefficient.	It varies from 0.003 to 0.006.
$\left(\frac{C_d}{C_l}\right)_{min}$	Minimum slope point, it corresponds to the airfoils' maximum lift-to-drag ratio.	
C_{m0}	Pitching moment coefficient: pitching moment coefficient about quarter chord. It is important to select the pitching moment coefficient as close to zero as possibly achievable.	Typical values are usually between -0.02 and -0.05.

At subsonic speeds the parameters summarized in Table 9 are affected by geometrical parameters of the airfoil mainly the camber, thickness ratio, Reynolds number, surface roughness and the critical Mach number. Table 10 summarizes the all these dependencies.

Table 10: Airfoil Geometrical and Aerodynamic Parameters Dependencies

Airfoil Geometrical Characterizing Parameter	Airfoil Aerodynamic Parameter Affected	Impact when Airfoil Geometrical Characterizing Parameter is Increased
Camber	Angle of zero lift C_{ol}.	More negative.
	Ideal (Optimum or Design) lift coefficient C_{li}.	Increases.
	Pitching moment coefficient C_{m0}.	More negative.
Thickness ratio	Minimum drag coefficient C_{dmin}.	Increases.
	Maximum lift coefficient C_{lmax}.	Highest for airfoil thicknesses ranging from 12 % to 16 %.
	Stall pattern.	Stall pattern is also Gradual for airfoil thicknesses ranging from 12 % to 16 %.
	Drag divergence Mach number (M_D).	Decreases.
	Wing structural weight.	Increases.
Reynolds Number	Minimum drag coefficient C_{dmin}.	Decreases.
	Maximum lift coefficient C_{lmax}.	Increases.
Surface roughness	Minimum drag coefficient C_{dmin}.	Increases.
	Maximum lift coefficient C_{lmax}.	Decreases.
Critical Mach number	Airfoil shape.	Old design versus supercritical airfoils (flat upper surface; have highest M_D).
	Thickness ratio.	Decreases.
	Lift coefficient.	Highest near C_{li}.

Definitions:

The drag divergence Mach number noted by MD above, is generally defined as the Mach number at which the drag coefficient shows an increase of 0.002 over the subsonic drag value. Some references defines the drag

divergence Mach number as the Mach number at which the slope of the drag coefficient versus Mach number curve has a value of 0.1 [4].

4.11.2. Selection Criterions

The following are the key criterions for selecting an airfoil that complies with design requirements.

a. Airfoil Maximum Thickness-to-Chord Ratio

Equation (39) provided in [12] in which the dependency between the relative thickness and the design Mach number are clearly illustrated for a two-dimensional flow. It yields pertinent values for subsonic wing design.

$$\left(\frac{t}{c}\right) = 0.30\left\{\left[1 - \left\{\frac{5+M^2}{5+(M^*)^2}\right\}^{3.5}\right]\frac{\sqrt{1-M^2}}{M^2}\right\}^{(2/3)} \tag{39}$$

In this equation, M denotes the design Mach number for which the airfoil is to be designed, often at cruise speed. For Swept wings, the Effective Mach Number calculated using Equation (40) is to be used.

$$M_{eff} = M\left(\cos\Omega_{1/4}\right)^{0.5} \tag{40}$$

The Factor M^* is a figure defining the aerodynamic sophistication employed to obtain supercritical flow at a design condition. Accurate results are obtained by considering the following:

- ❖ $M^* = 1.00$; for conventional airfoils; maximum relative thickness at about 0.30 time Chord length.
- ❖ $M^* = 1.05$; High-speed (Peaky) airfoils, 1960-1970 technology.
- ❖ $M^* = 1.12$ to 1.15; for supercritical airfoils.

The derivation for Equation (39) is given in [13]. For more details on the subject, [14] presents the results of a literature review with further development of the covered equations.

For guidance, the typical values for the airfoil relative airfoil thickness for subsonic aircraft are as follow [6]:

- ❖ For a low speed aircraft with a high lift requirement (i.e. cargo aircraft), the typical wing relative thickness ranges from 15 % to 18 %.
- ❖ For a high speed aircraft with a low lift requirement (i.e. high subsonic passenger aircraft), the typical wing relative thickness ranges from 09 % to 12 %.

b. Airfoil Maximum Lift Coefficient

The general lift equation implies that for any given aircraft weight, the lift coefficient is inversely proportional with the square of the airspeed. As such, in order to sustain aircraft weight in the air; higher lift coefficient is necessary at low speed and lower lift coefficient is necessary at higher speed, this infers that higher lift

coefficient results in a safer flight.

The lift coefficient is a function of the angle of attack, it increases till it reaches its maximum at the stall angle. The stall speed of an aircraft is determined by the wing loading at maximum weight often at takeoff and the maximum wing lift coefficient computed at sea level in hot day. The airfoil maximum lift coefficient is directly proportional to the wing maximum clean lift coefficient. The term `` clean ʺ defines the wing lift coefficient without the deployment of high lift devices. The use of high lift systems is necessary to achieve the high lift coefficients required on takeoff and landing. Equation (41) is used to compute the maximum wing lift coefficient, for a given stall speed, takeoff weight and wing area.

$$C_{L_{max}} = \frac{2.g.W_0}{\rho_0.S.V_s^2} \qquad\qquad (41)$$

Where,

- ❖ g: Gravity 9.81 $m/_{s^2}$.
- ❖ S: Total wing area in m^2.
- ❖ V_s: Stall speed in $\frac{m}{s}$.
- ❖ ρ_0: Air density at sea level, $\rho_0 = 1.225 \frac{Kg}{m^3}$.
- ❖ W_0: Takeoff mass in Kg.

The design specifications for military and civil aviation defines the maximum acceptable stall speeds for different classes of aircrafts.

The approach speed (V_A) is the speed at which the aircraft approaches a runway for landing.

The approach speed is either explicitly stated in the design requirements or selected based on the approach category of the aircraft, which constitutes a grouping that differentiate aircrafts based on their approach speeds. The criteria considers the aircraft approach speed in the landing configuration (flaps and gear deployed) at the maximum certified mass as summarized in Table 11.

Table 11: Aircraft Approach Categories

Category	V_A (Km/h)	V_A (Knots)	Aircraft Class	Examples
A	$V_A < 169$	$V_A < 91$	Small single engine	Baron G58
B	$169 \leq V_A < 224$	$91 \leq V_A < 121$	Small multi engine	Saab 2000, Embraer 120
C	$224 \leq V_A < 261$	$121 \leq V_A < 141$	Airline jet/Cargo	B737, C-130, A320, F100
D	$261 \leq V_A < 307$	$141 \leq V_A < 166$	Large jet/military jet	B747, L-1011, MD-11, A340
E	$307 \leq V_A < 391$	$166 \leq V_A < 211$	Unusual/Special military	Concorde, Tu144

Design requirements and specifications regulations define the approach speeds as multiples of the stall speeds. Typical multipliers are summarized in Table 12.

Table 12: Approach Speed Multiples

$V_a \geq K.V_s$	
Aircraft Category	**Typical Values for K**
Civilian Aircraft	1.30
Military Aircraft	1.20
Carrier Based Aircraft	1.15

To get a better picture on the typical values for the maximum lift coefficient, Table 13 summarizes some wing models. The first being a wing a simple plain wing, whereas the others are equipped with different high-lift devices.

Table 13: Typical Values for the Maximum Lift Coefficients

Wing Model	**Typical Maximum Lift Coefficients**
Plain wing	$1.2 \leq C_{Lmax} \leq 1.5$
Wings with inner flaps	$1.6 \leq C_{Lmax} \leq 2.0$
Wings with large flaps	C_{Lmax} could reach 5.0
Short Take Off and Landing (STOL)	C_{Lmax} around 3.0
Transport aircraft with flaps and slats	C_{Lmax} around 2.4

To estimate the airfoil maximum lift coefficient, it is important to evaluate the wing maximum clean lift coefficient first, this is accomplished using Equation (42).

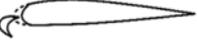$$C_{Lmax_{clean}} = C_{L\,max} - \Delta C_L \qquad (42)$$

Where,

❖ ΔC_L: High-lift system lift increment.

Table 14 provides values for lift increment depending on the high-lift device used. When using Equation (42), average values are to be used.

Table 14: Typical Values for the Maximum Lift Coefficients [6]

Nº	High Lift Device	Description	ΔC_L	
Training Edge High Lift Device or Flap (TEHLD)				
1	Plain Flap	It is an airfoil shape that is hinged at the wing trailing edge such that it can be rotated, only the downward deflection is considered.	0.7 0.9	-
2	Split Flap	Only the bottom surface of the flap is hinged so that it can be rotated downward.	0.7 0.9	-
3	The Single Slotted Flap.	Similar to a plain flap, except the following: ❖ Its leading edge is carefully designed such that it modifies and stabilizes the boundary layer over the top surface of the wing. ❖ It moves rearward during the deflection, this increases the effective chord.	1.0 1.3	-
4	Double Slotted Flap	It is similar to a single slotted flap, except it has two slots; it is divided into two segments, each with slots.	$1.3\frac{c_f}{c}$	
5	Triple Slotted Flap	It is an extension to a double slotted flap, it has three slots.	$1.6\frac{c_f}{c}$	
6	Fowler Flap	It has a special mechanism that deflects the flap downward and tracks it to the trailing edge of the wing.	$1.9\frac{c_f}{c}$	
Leading Edge High Lift Device (LEHLD)				
7	Leading Edge Flap	This flap is similar to trailing edge plain flap, except it is installed at the leading edge of the wing. The leading edge pivots downward and the gap between the flap and the main wing body is sealed with an increase in the effective camber.	0.2 0.3	-
8	Leading Edge Slat	It is a small, highly cambered section located slightly forward of the leading edge the wing body. When deflected, a slat is basically a flap at the leading edge, but with an unsealed gap between the flap and the leading edge.	0.3 0.4	-
9	Kruger Flap	This leading edge high lift device is essentially a leading edge slat which is thinner, and which lies flush with the bottom surface of the wing when not deflected.	0.3 0.4	-

In the above table, the fraction $\frac{c_f}{c}$ denotes the ratio between the chord of high-lift device to the chord of the main wing body as illustrated in Figure 13.

Equation (43) is the semi-empirical relationship [15] used to estimate the optimum outer panel airfoil maximum lift coefficient.

$$C_{l\,max} = \frac{C_{Lmax_{clean}}}{(0.86 - 0.002\,\Omega_{LE})} \qquad (43)$$

Where,

❖ Ω_{LE}: Leading edge sweep angle in degrees.

The use of high-lift devices is not only incrementing the wing lift, but also impacts the zero-lift angle. Equation (44) is an empirical expression [6] that provides the zero-lift angle of attack incremental ($\Delta\alpha_0$) as a function of flap-to-wing-chord ratio and flap deflection angle.
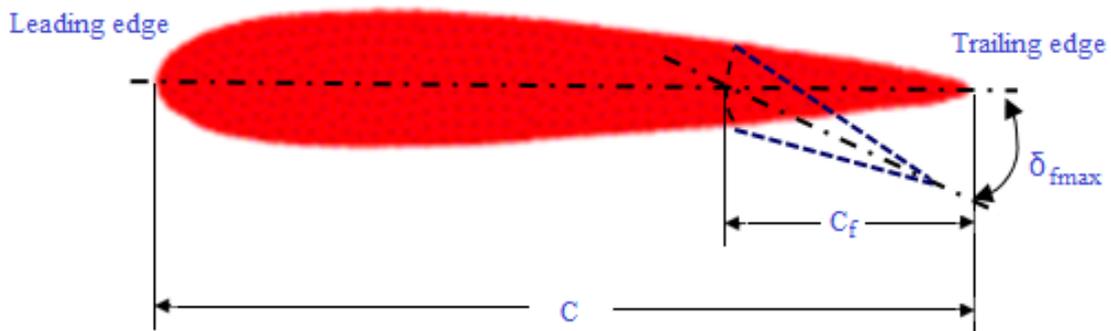

Figure 13: High-Lift Device Parameters

$$\Delta\alpha_0 \approx -1.15\frac{c_f}{c}\delta_f \qquad (44)$$

Where,

❖ δ_f: Flap deflection angle.

c.   *Airfoil Ideal or Design Lift Coefficient*

Cruising at altitude is the foremost segment of a typical conventional flight mission profile, it is the section in which the aircraft spends most of its time. At cruise or level flight the generated lift must equal the aircraft weight. The best cruise flight strategy that maximizes the aircraft travelled range, is often to fly at constant cruise velocity (V_c) with a slightly positive flight path at constant angle of attack. In these conditions, the required average wing lift coefficient could be calculated using Equation (45).

$$C_{L_C} = \frac{2.g.\overline{W}}{\rho_c.S.V_c^2} \qquad (45)$$

Where:

❖   g: Gravity 9.81 $^m/_{s^2}$.
❖   S: Total wing area in m^2.

❖ V_c: Cruise speed in $\frac{m}{s}$.

❖ ρ_c: Air density at cruise altitude.

❖ $\overline{W}$: Cruise segment average mass in Kg.

The air density at a given altitude (h) in standard conditions could be estimated using Equation (46).

$$\rho_h = \begin{cases} 1.225 * (1 - 2.2558 * 10^{-5} * h)^{4.2559} & \text{for h } < 11000 \text{ m} \\ 0.3639 * \exp\left(\frac{(11000-h)}{6341.5987}\right) & \text{for h } \geq 11000 \text{ m} \end{cases} \tag{46}$$

The best estimate of mean weight [16] for a given cruise segment is calculated using Equation (47).

$$\overline{W} = \sqrt{W_{ini}.W_{fin}} \tag{47}$$

Where:

❖ W_{ini}: Aircraft's weight at the start of the cruise segment in Kg.

❖ W_{fin}: Aircraft weight at the end of the cruise segment in Kg.

The airfoil ideal lift coefficient (C_{l_i}) is predicted based on the average wing lift coefficient (C_{L_c}), the first approximation is based on Equation (48).

$$C_{l_i} = 0.9 \cdot C_{L_c} \tag{48}$$

Equation (48) states that from design point of view, the objective is to cruise at flight situation such that the wing cruise lift coefficient is as close as possible to the ideal (optimum) lift coefficient of the airfoil. In other words, the design lift coefficient must be the one at which the airfoil has the minimum drag as illustrated in Figure 12. The camber is the geometrical parameter that defines the airfoil optimum lift coefficient.

d. *Airfoil lift-to-drag ratio*

Many aircraft, such as the Myasishchev M-55 and Lockheed U-2, which are designed for reconnaissance or spying require high endurance characteristics. When the time spent in the air is the main interest and not the distance traveled then the design concern is loiter time or endurance.

The maximum endurance of an aircraft is defined as the flight condition that requires the minimum fuel power. This flight condition is achieved through the maximization of the lift-to-drag ratio by selecting the wing cruise lift coefficient as close as possible to the airfoil lift coefficient that yields minimum drag-to-lift ratio (maximum lift-to-drag ratio) as illustrated in the drag polar plot on Figure 12. Geometrically, this is the point on the airfoil drag polar plot that is tangent to a line from the origin and closest to the vertical axis.

e. *Airfoil Lift Curve Slope*

The lift curve slope is significant performance piece of an airfoil. The key function of the airfoil is the generation of lift, as such the higher the lift slope the better is the airfoil. The ideal value of lift curve slope of an airfoil is 2π radians or 0.16 per degrees. Equation (49) is an empirical expression [4] used to estimate the lift curve slope per radians.

$$C_{l\alpha} = 1.8\pi \left(1 + 0.8 \left(\frac{t}{c}\right)_{max} \right) \tag{49}$$

Where:

❖ $\left(\frac{t}{c}\right)_{max}$: Airfoil maximum thickness-to-chord ratio estimated using Equation (39).

f.   Airfoil Pitching Moment Coefficient

In aircraft aerodynamics, the pitching moment on an airfoil is the moment or torque produced by the aerodynamic force on the airfoil [17]. The pitching moment is measured about the aerodynamic center of the airfoil. At subsonic speeds, the aerodynamic center usually lies around a quarter chord from the wing leading edge. The quarter chord pitching moment coefficient does not vary significantly over the operating range of angle of attack.

The total wing pitching moment about the aerodynamic center is largely dependent on the airfoil pitching moment. The wing pitching moment of an aircraft is a portion of the total pitching moment that must be equalized using the horizontal stabilizer. The size optimization of the horizontal tail and the reduction of aircraft gross weight is achieved by lowering the wing pitching moment. In other words, it is important to select an airfoil with the lowermost (close to zero) negative or positive pitching moment.

g.   Stall Pattern Quality

The stall quality illustrated in Figure 11 is another important airfoil characteristic, it is basically the shape of the lift curve beyond the stall angle. Even though the abrupt airfoil stall behavior does not necessarily imply wing stall; it is preferable to use an airfoil with a smooth and slow drip in lift, rather than a sudden and fast lift loss beyond the stall angle. Airfoils with high thickness or camber are characterized by a gradual loss of lift but with a lower maximum lift coefficient.

h.   The Challenge

It is not easy to find an airfoil that encloses optimum values for all the above requirements. Usually, the selection process is done through a weighing process that compromises a feature over another depending of the fight requirements. As mentioned previously, only large aircraft manufacturer could design airfoils that encompasses all the needed design aspects.

4.11.3. NACA Airfoils

The NACA airfoils are a collection of airfoil shapes developed by the National Advisory Committee for Aeronautics. Each airfoil is described using a series of digits following the word "NACA" The parameters in the numerical code could be entered into equations to precisely generate the cross-section of the airfoil and calculate its properties. The three main interesting groups of NACA airfoils are summarized in Table 15.

Table 15: Typical Values for the Maximum Lift Coefficients [18]

Family	Description	Advantages / Disadvantages	Applications
4-Digit	1. First digit: Maximum camber as percentage of the chord. 2. Second digit: Distance of maximum camber from the airfoil leading edge in tens of percent of the chord. 3. Last two digits: Maximum thickness of the airfoil as percent of the chord.	1. Low maximum lift coefficient. 2. Relatively high drag. 3. High pitching moment. 1. Good stall characteristics. 2. Small center of pressure movement across large speed range. 3. Roughness has little effect.	1. General aviation. 2. Horizontal tails. Symmetrical: 1. Supersonic jets. 2. Helicopter blades. 3. Shrouds. 4. Missile/rocket fins.
5-Digit	1. First digit: When multiplied by 0.15, gives the lift coefficient. 2. Second and third digits: When divided by 2, give the distance of maximum camber from the leading edge as per cent of chord. 3. Fourth and fifth digits: Maximum thickness of the airfoil as per cent of the chord.	1. Higher maximum lift coefficient. 2. Low pitching moment. 3. Roughness has little effect. 1. Poor stall behavior. 2. Relatively high drag.	1. General aviation. 2. Piston-powered bombers, Transports. 3. Commuters. 4. Business jets.
6-Series	1. First digit: Number "6", it indicates the series. 2. Second digit: Distance of the minimum pressure area in tens of percent of chord. 3. Third digit: The subscript digit; range of lift coefficient in tenths above and below the design lift coefficient. 4. A hyphen. 5. Fourth digit: Design lift coefficient in tenths. 6. Last two digits: Maximum thickness in tens of percent of chord.	1. High maximum lift coefficient. 1. High drag outside of the optimum range of operating conditions. 2. High pitching moment. 3. Poor stall behavior. 4. Very susceptible to roughness. 5. Very low drag over a small range of operating conditions 6. Optimized for high speed	1. Piston-powered fighters. 2. Business jets. 3. Jet trainers. 4. Supersonic jets.

Examples:

NACA 2414:

❖   Maximum camber: 02 %

❖   Maximum camber location: 40 % from the leading edge.

❖   Maximum thickness: 12 % of the chord.

NACA 0015:

❖ Symmetrical airfoil.

❖ Maximum camber: no camber.

❖ Maximum thickness: 15 % of the chord length.

NACA 12045:

❖ Lift Coefficient: 0.15

❖ Maximum camber location: 10 % from the leading edge.

❖ Maximum thickness: 45 % of the chord.

NACA 61_2-345:

❖ Minimum pressure area distance: 10 % of the chord back.

❖ Range of lift coefficient: Maintains low drag 0.2 above and below the lift coefficient.

❖ Design lift coefficient: 0.3.

❖ Maximum thickness: 45 % of the chord.

4.12. Twist Angle

The twist is primarily used to prevent tip stalling. Tip stalling is a phenomenon in which the wing stall begins in the region near the wing tips. This occurs because the wing lift distribution on the wing is higher in the region near the wing tips. Consequently, when the angle of attack increases the lift distribution at the tips exceeds the maximum lift coefficient causing the early stall of the wing tip region over the wing root region.

Wing Ailerons are located in the tip region, they are of a great importance in spin recovery which often occurs after stall. The ailerons effectiveness in a stall event would be possible only if the air flow over the wing outboard section is kept healthy. Twist is an important tool used for revising the lift distribution to an elliptical one as illustrated in Figure 14.

Twisting a wing could be achieve either geometrically or aerodynamically. Aerodynamic twist is implemented by using airfoil sections with different zero-lift angles along the span (changing the airfoil camber). On the other hand, geometric twist is achieved, by using an identical airfoil from root to tip while lowering the angle of attack. In practice, the application of aerodynamic twist is more suitable than the geometric twist.

Large amount of twist, usually much over 5 degrees is avoided, this is because the twist optimization is done for a particular aircraft flying condition such as cruise. Therefore, lift distribution revision is done for a particular lift coefficient, while ensuring an optimum wing efficiency at other lift coefficients or flying conditions. The twist optimization is done by selecting the twist angle that allows tips stalling after the roots while providing an elliptical lift distribution.
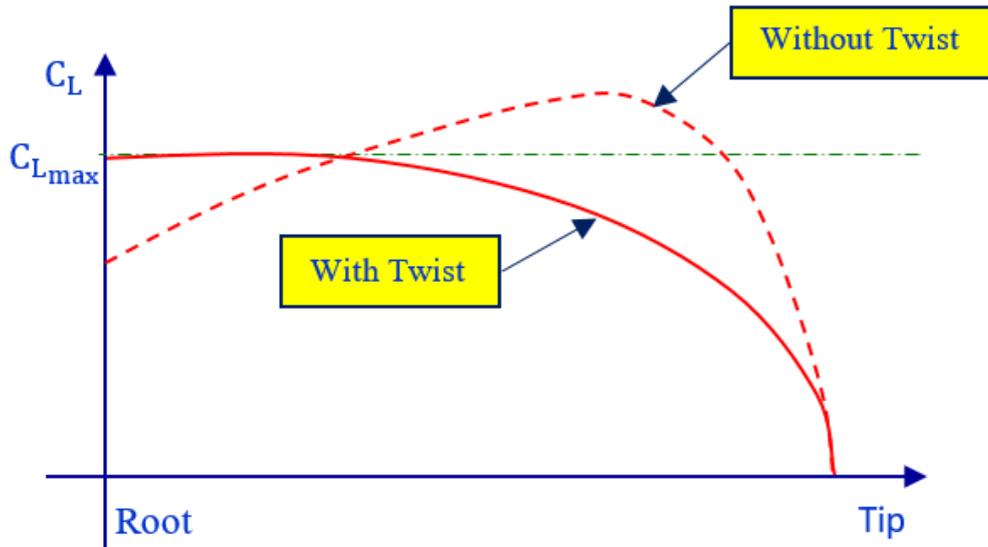
Figure 14: Lift distribution Over the Half Wing With and Without Twist

It is important to consider that fact that if high wing twist angle would result in a negative lift in the outer wing section. The criterion formulated in Equation (50) must be respected when selecting the wing twist angle to avoid generation of negative lift.

$$|\alpha_t| + i_w \geq |\alpha_0| \tag{50}$$

Where:

❖ α_t: Wing twist angle.

❖ i_w: Wing incidence (setting) angle, covered in the next section.

❖ α_0: Wing zero-lift angle of attack (assumed the same as the airfoil).

The typical value for the geometric twist is between -1 and - 4 degrees. Generally a value of -3 degrees provides satisfactory stall characteristics [2].

4.13. Wing Setting Angle

The aircraft spends most of its flight at cruise where the drag is at minimum, thus allowing economy in fuel consumption. To achieve a minimum drag at cruise, the aircraft fuselage must be at zero angle of attack. To sustain the aircraft weight in the air, the wing is mounted on the fuselage with a pre-set angle of attack that allows production of the required lift. The angle between fuselage reference line and the wing reference line is called wing incidence angle (i_w).

The wing incidence could be estimated using Equation (51).

$$i_w = \frac{C_{L_c}}{C_{L\alpha}} + \alpha_0 \tag{51}$$

Where:

- ❖ α_0: Wing zero-lift angle of attack (assumed the same as the airfoil).
- ❖ $C_{L\alpha}$: Wing lift slope coefficient, estimated using Equation (24).
- ❖ C_{L_c}: Average wing lift coefficient at cruise, estimated using Equation (45).

The final choice of the wing setting angle is done through simulations and established by means of wind tunnel tests on the aircraft model. Typical values for the different classes of aircraft are summarized in Table 16.

Table 15: Typical Incidence Angles [2]

Aircraft Class	Typical Incidence Angle
General aviation and home built	2º
Transport	1º
Military	0º

5. OpenVSP Software

OpenVSP is a parametric aircraft geometry tool. OpenVSP allows the user to create a 3D model of an aircraft defined by common engineering parameters. This model can be processed into formats suitable for engineering analysis [19].

OpenVSP is the tool used to analyze the designed wings in the objective of validating the approach proposed in this paper.

6. Design Examples

6.1. Military Strategic Jet Airlifter

Design Requirement:

- ❖ Crew: 5.
- ❖ Payload: 42 Tons.
- ❖ Cruise Speed: $900 \frac{Km}{h}$ (Mach 0.82).
- ❖ Range: 5,000 Km.
- ❖ Loiter Time: 1 hour.
- ❖ Engine Type: High-bypass Turbofan.
- ❖ Engine Specific Fuel Consumption: $16.85 \left[\frac{g}{KN/s} \right]$

The primary step to consider in response to the design requirements, would be to select an appropriate conceptual approach. The overall profile of any aircraft is described by defining its fuselage, wing, tail and

canard features. For this mission, a conventional approach has been selected as follows:

Fuselage:

The aircraft is a military strategic airlifter, thus the cargo compartment floor must be close to ground generally around 1.5 meters to allow direct loading and unloading of cargo from or to the aircraft especially in unaccommodated areas.

The cross section of the cargo compartment is also very important, it must be sized to carry some outsized cargos such as tanks and trucks.

The rear-loading will be adapted, an aft-fuselage upsweep of about 15 degrees is acceptable, this is also important for reducing the drag.

The subsonic drag is also minimized by selecting a minimum fitness ratio of about 3.0, this is the ratio between the fuselage length and its maximum cross-sectional area equivalent diameter. For cargo aircrafts, a typical value would be 8. Moreover, the landing gears are designed retractable, thus the fuselage must have undercarriage space to accommodate them, this will also contribute in the overall parasitic drag reduction.

Wing:

The high wing position is carefully chosen as it facilitates the loading and unloading of the cargo. In addition, the engines are easily installed below the wing. Considering the cargo weight, it is expected a prerequisite for a power plant composed of 04 engines. Furthermore, this design offers a lower possibility of human accident to be pulled to the engines inlets. Last but not least, it offers more space inside fuselage for cargo.

To make sure the wing generates the required lift at takeoff and landing with such high cargo weights, it will be equipped with single slotted flaps and leading edge slats.

Tail:

A T-Tail configuration is more adequate for this design. It reduces fatigue for both structure and pilot especially for the 42 Tons cargo and 5,000 Km distance to travel. Furthermore, it allows a smaller vertical tail thanks to the end-plate effect. Last but not least, its horizontal tail is cleared from the wing wake making it efficient and reduced in size.

Canard:

No canard is used in this approach.

This example illustrates the importance of the proper selection of the conceptual approach to be used before performing any advanced analysis on the aircraft. Figure 15 exposes the proposed sketch derived based on the above descriptions to fit the mission requirements.

Figure 15: Military Strategic Airlifter Proposed Sketch

As per Table 8, the targeted equivalent skin coefficient for military cargo aircrafts with low upsweep fuselage would be between 0.0030 and 0.0035. The aircraft belongs to category D, an approach speed of 150 Knots has been selected for this design. Convergence has been achieved at a skin friction coefficient of 0.0031 following the flowchart illustrated in Figure 4 with the following parameters: aspect ratio = 8.36, wetted area ratio = 6.5, maximum lift to drag ratio = 16, wetted aspect ratio = 1.29 and takeoff wing loading = $550 \frac{\text{Kg}}{\text{m}^2}$ (loading index = 6.915). Table 16 summarizes the obtained results. The aircraft will cruise at an altitude of 11,400 meters with full load and its takeoff weight is 133.627 Tons.

Table 16: Military Strategic Jet Airlifter Design Summary (Cyan: entered data, Yellow: computed values)

Nº	Parameter	Values and Units					Reference or Comment
		Postulated Aerodynamic Features					
1	Equivalent Aspect Ratio	6,89					Table 2, a= 5,57 and C=-1,075.
2	Actual Aspect Ratio	8,36					Point 4.2, Equivalent one divided by 0.825.
3	Selected Wetted Area Ratio (Swet/Sref)	6,50					Eyeball estimated using Figure-9.
4	Computed Wetted Aspect Ratio	1,29					Equation (21).
5	Maximum Lift-to-drag ratio	16,00					Figure 9, Military Jets.
6	Lift-to-drag ratio at Cruise	13,86					Table 7, Jet at cruise.
7	Lift-to-drag ratio at Loiter	16,00					Table 7, jet at Loiter.
		Engine and Performance					
1	Specific Fuel Consumtion at Cruise (1/h)	0,596	0,00016556	(1/s)			Equation (16) and Equation (18).
2	Specific Fuel Consumtion at Loiter (1/h)	0,477	0,00013244	(1/s)			Table 5 at 80 % SFC at Cruise.
3	Required Range (Km)	5 000,00	5 000 000	(m)			Convert Range to meters.
4	Cruise Speed (Mach)	0,82	271,80	(m/s)	1 012,54	(Km/h)	Conversion to m/s and Km/h.
5	Loiter Time (Min)	60,000	3 600,00	(s)			Conversion from hours to Seconds.
		Mission Segments Weights Fractions					
1	Empty Weight Fraction - Coefficient A	0,93					Table 3, Military Cargo / Bomber.
2	Empty Weight Fraction - Coefficient C	-0,07					Table 3, Military Cargo / Bomber.
3	Empty Weight Fraction - Coefficient K	1,00					Table 3, Fixed sweep wing.
4	Fuel Fraction - Warmup and Takeoff	0,970					Table 4.
5	Fuel Fraction - Climb	0,985					Table 4.
6	Fuel Fraction - Jet Cruise Segment	0,803					Equation (13).
7	Fuel Fraction - Jet Loiter Segment	0,971					Equation (14).
8	Fuel Fraction - Landing	0,995					Table 4.
9	Total Fuel Fraction with 6 % allowance - Jet	0,275					Equation (19) and (20)
		Mission Segments Weights					
1	Aircraft Takeoff Weight (Kg)	133 627,0					Iterative solving of Equation (12)
2	Aircraft Empty Weight (Kg)	54 395,7					Table (3) using Takeoff Weight and Coefficients above.
3	Crew Weight (Kg)	500,0					05 crew members, with 100 Kg each , this makes it 500 Kg.
4	Payload Weight (Kg)	42 000,0					From design requirements.
5	Total Fuel Weight (Kg)	36 731,3					Iterative solving of Equation (12), then use weight fraction above.
6	Aircraft Weight - End of Warmup and Takeoff (Kg)	129 618,2					Weight at the end of the Warmup and Takeoff segment.
7	Aircraft Weight - End of Climb (Kg)	127 673,9					Weight at the end of the Climb segment.
8	Aircraft Weight - End of Jet Cruise Segment (Kg)	102 481,1					Weight at the end of the Cruise Segment segment.
9	Aircraft Weight - End of Jet Loiter Segment (Kg)	99 472,3					Weight at the end of the Loiter Segment segment.
10	Aircraft Weight - End of Landing (Kg)	98 974,9					Weight at the end of the Landing segment.
11	Reserves and Trapped Fuel - 6 % Allowance (Kg)	6 088,0					Weight of the 6 % fuel allowance.
12	Average Cruising Weight (Kg)	114 386,1					Equation (47), using End of Climb and End of Cruise Weights.

Table 16: Military Strategic Airlifter Design Summary (Cont'd)

Nº	Parameter	Values and Units				Reference or Comment
		Wing Parameters				
1	Takeoff Wing Loading Index	6,915				Figure 5, Value of wing loading is seletced between 6 and 8.
2	Takeoff Wing Loading (Kg/m2)	550,2				Equation (8).
3	Wing Leading Edge Sweep Angle (deg)	28,7	0,5006	(rad)		Equation (9), using method described in Point 4.4.
4	Wing Area (m2)	242,89				Equation (22).
5	Wing Span (m)	45,06				Equation (2).
6	Taper Ratio	0,18				Equation (10), using method described in Point 4.4.
7	Root Chord (m)	9,13				Equation (4).
8	Tip Chord (m)	1,65				Equation (3).
9	Quarter Chord Sweep (deg)	24,90	0,4346	(rad)		Equation (10), using method described in Point 4.4.
10	Mean Chord Length (m)	6,3				Equation (6).
11	AC Distance from Fuselage (m)	8,7				Equation (7).
12	AC Distance from Leading Edge (m)	1,6				Descriptive Text in Point 2.
13	Total Wetted Area(m2)	1 578,78				Description in Point 4.5.3.
14	Wing Zero Lift Angle (deg)	-1,25				Point 4.13.
15	Wing Incidence Angle (deg)	2,31				Equation (51).
		Aircraft Main Speeds				
1	Approach Speed (Knots)	150,0	77,17	(m/sec)	277,80 (Km/h)	Conversion to m/s and Km/h.
2	Min. Approach to Stall Coefficient	1,2				Table 12
3	Stall Speed (Knots)	125,0	64,3	(m/sec)	231,50 (Km/h)	Conversion to m/s and Km/h.
4	Cruise Altitude (m)	11 400,0				Conversion to m.
5	Air Density at Cruise Altitude (Kg/m3)	0,3417				Equation (46).
6	Air Density at Sea Level (Kg/m3)	1,2250				Equation (46) at zero meters.
		Lift Coefficients				
1	Maximum Lift Coefficient	2,13				Equation (41).
2	HLD Lift Coefficient Increment ΔCL	1,45				Table 14, Single slotted flap (1.15) + leading edge slat (0.3) = 1.45.
3	Maximum Clean Lift Coefficient CLmax	0,68				Equation (42).
4	Cruise lift Coefficient	0,37				Equation (45).
5	Lift Slop Coefficient CLα (1/rad)	5,89	0,1028	(1/deg)		Equation (24).
		Calculated Aircraft Aerodynamic Features				
1	Oswald efficiency Factor ε	0,771				Equation (25).
2	Drag-due-to-Lift factor K	0,049				Equation (26).
3	CDo at Max(L/D)	0,0199				Equation (28), solved for CD_0.
4	Cruise Drag Coefficient	0,026				Equation (29).
5	Loiter Lift Coefficient	0,63				Equation (31).
6	Loiter Drag Coefficient	0,040				Equation (32).
7	Lift-to-drag ratio at Cruise	13,85				Computed lift-to-drag ratio at cruise using Equation (27).
8	Lift-to-drag ratio at Loiter	15,97				Computed lift-to-drag ratio at Loiter using Equation (30).
9	Cfe Subsonic	0,0031				Equation (23).
		Airfoil Calculated Features				
1	Effective Mach Number (Mach)	0,78				Equation (40).
2	Aerodynamic Sophistication Figure Factor M*	1,00				Conventional airfoils.
3	Wing airfoil thickness t/c	0,107	10,7%	(%)		Equation (39).
4	Airfoil Ideal Lift Coefficient Cli	0,33				Equation (48).
5	Airfoil Maximum Lift Ceofficient Clmax	0,85				Equation (43).
6	Airfoil lift curve slope C_l_alpha	6,139	0,1028	(1/deg)		Equation (49).

Based on the resulting parameters, Figure 16 provides an overview on the obtained aircraft weights allotment.

Figure 16: Obtained Weight Allotment - Jet Airlifter

Simulation Using OpenVSP:

Figure 17 illustrates the 3D-view of the obtained wing based on the wing parameters summarized in Table 16. Notice that no fuselage is illustrated in this case, only the wing is demonstrated. The analysis has been done at cruise condition.
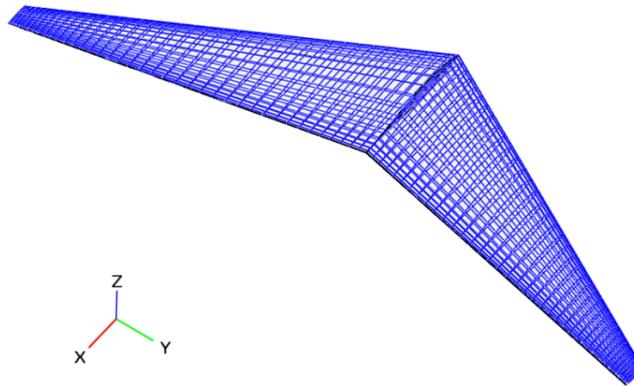

Figure 17: OpenVSP 3D-View of the Obtained Wing

To meets the design requirements, a NACA 6-Digit airfoil is synthetized based on the description in Table 15, the airfoil would be the NACA 63_2-311 illustrated in Figure 18. Airfoil selection technicalities are detailed in Section 4.11.
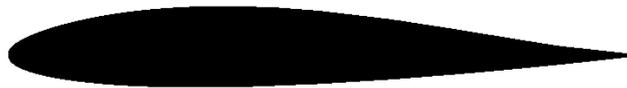

Figure 18: Illustration of the NACA 63_2-311

As illustrated in Figure 19, the OpenVSP Simulation, corrected the wing incidence angle at cruise to zero degrees. At this angle the wing pitching moment along the X-Axis is zero.
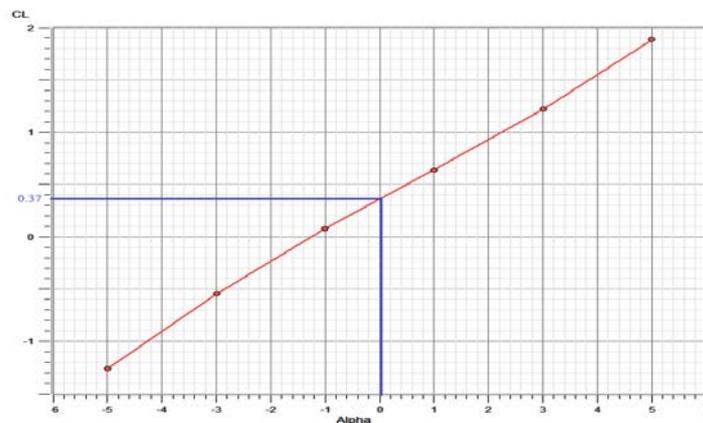

Figure 19: Wing Lift Coefficient versus Wing Incidence Angle

Figure 20 illustrate the yielded wing lift coefficient distribution, it is a tolerable practical elliptical distribution that correlates well with the computed Oswald efficiency factor of 0.77.

A geometrical twist angle of -1.5 degrees has been applied to the wing, it is the best angle that yields zero lift coefficient at the tips of the wing.
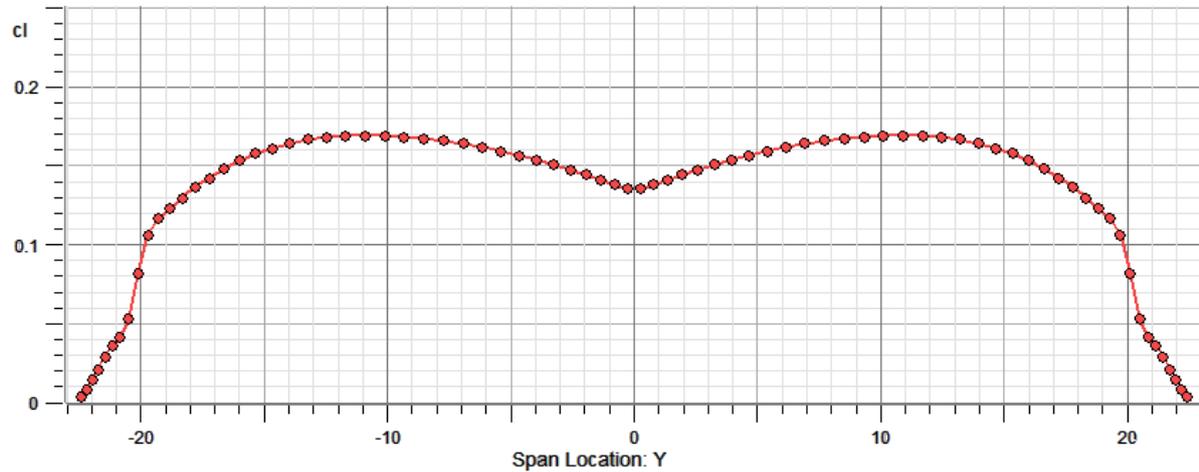

Figure 20: Wing Lift Coefficient Distribution

Figure 21 shows the mean-chord normalized load distribution. It is also an elliptical-like distribution. The load distribution is higher at to the root chord and decreases moving toward to the wing tip.
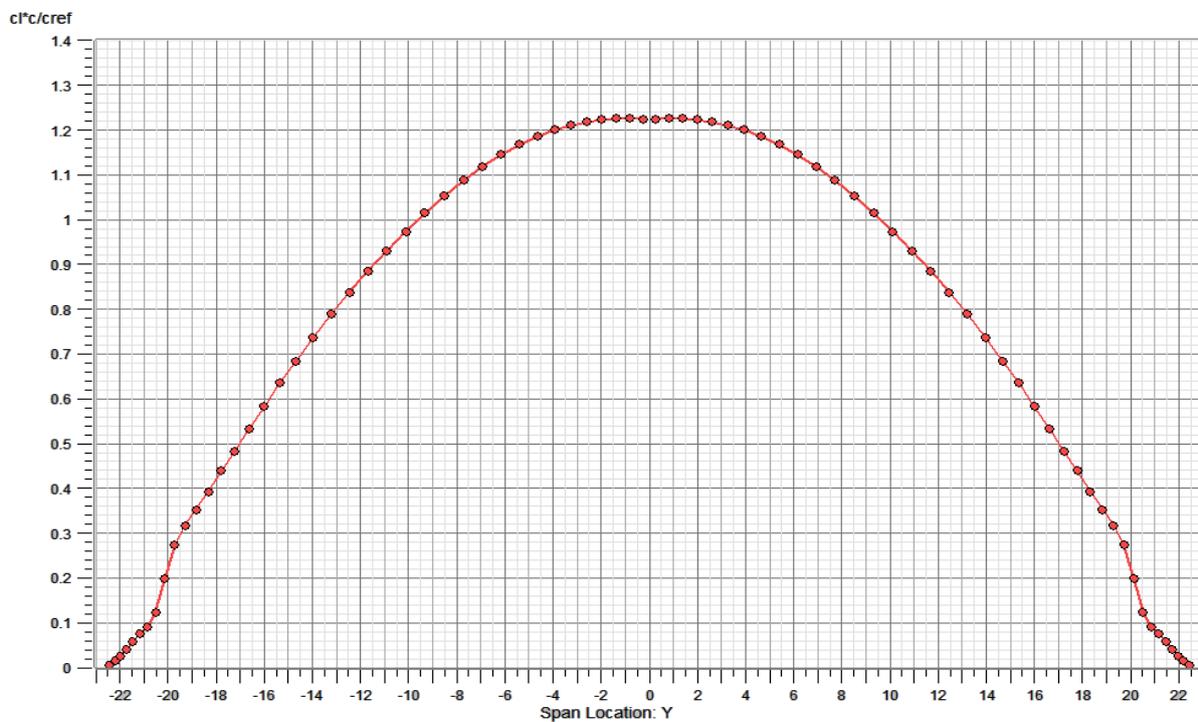

Figure 21: Normalized Wing Load Distribution

Figure 22 outlines the obtained pressure coefficient difference (Delta-CP) spreading over the wing. The pressure coefficient difference is well distributed, smooth and uniform span-wise and chord-wise, this ratifies the obtained elliptical lift and load distributions.
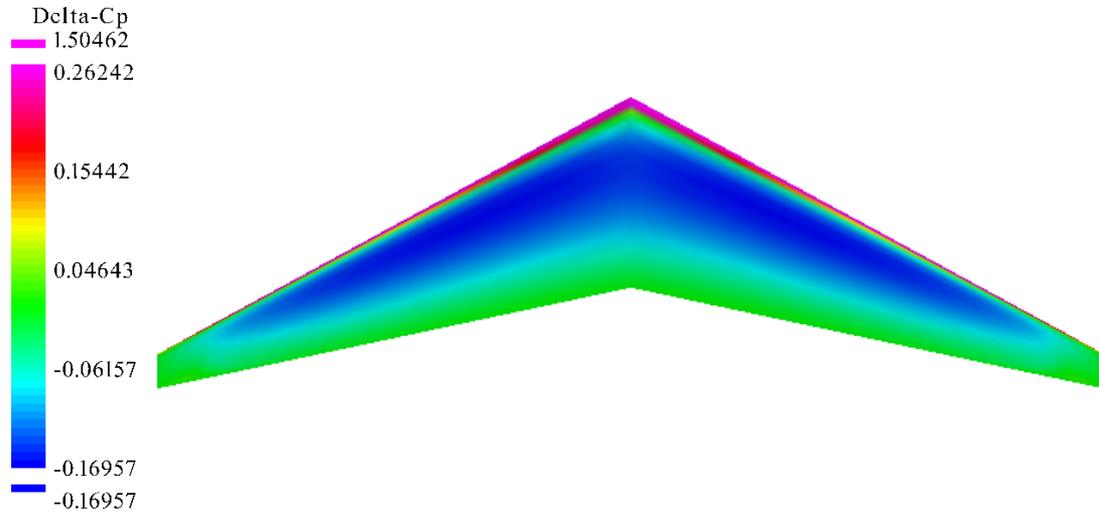

Figure 22: Pressure Coefficient Difference (Delta-CP) Distribution

6.2. *Military Strategic Turboprop Airlifter*

For this second example, some requirements from the first proposed design are revised. The altered design needs are summarized below:

- ❖ Payload: 20 Tons.
- ❖ Cruise Speed: $650 \frac{Km}{h}$ (Mach 0.526).
- ❖ Range: 3,500 Km.
- ❖ Engine Type: Turboprops.
- ❖ Brake Specific Fuel Consumption :$0.4455 \left[\frac{lb}{hp/h}\right]$

The first step would be to convert the brake specific fuel consumption to the equivalent jet engine specific fuel Consumption, this is achieved using Equation (15) at cruise speed with a propeller efficiency $\eta_p = 0.8$, this yields a Cruise SFC of $0.6\frac{1}{h}$ and using Table 6 the associated Loiter SFC is $0.720 \frac{1}{h}$.

As per Table 8, the targeted equivalent skin coefficient for this aircraft would be between 0.0045 and 0.0065. The aircraft belongs to category C, an approach speed of 130 Knots has been selected for this design. Convergence has been achieved at a skin friction coefficient of 0.0053 following the flowchart illustrated in Figure 4 with the following parameters: aspect ratio = 10.3, wetted area ratio = 6.02, maximum lift to drag ratio = 14.3, wetted aspect ratio = 1.71 and takeoff wing loading = $450 \frac{Kg}{m^2}$ (loading index = 6.413). Table 17 summarizes the obtained results. The aircraft will cruise at an altitude of 12,900 meters with full load and its

takeoff weight is 128.645 Tons.

Table 17: Military Strategic Turboprop Airlifter Design Summary

Nº	Parameter	Values and Units					Reference or Comment
		Postulated Aerodynamic Features					
1	Equivalent Aspect Ratio	8,50					Table 2, Propeller Aircraft.
2	Actual Aspect Ratio	10,30					Point 4.2, Equivalent one divided by 0.825.
3	Selected Wetted Area Ratio (Swet/Sref)	6,02					Eyeball estimated using Figure-9.
4	Computed Wetted Aspect Ratio	1,71					Equation (21).
5	Maximum Lift-to-drag ratio	14,30					Figure 9, Retractable Prop Aircraft.
6	Lift-to-drag ratio at Cruise	14,30					Table 7, Propeller at cruise.
7	Lift-to-drag ratio at Loiter	12,38					Table 7, Propeller at Loiter.
		Engine and Performance					
1	Specific Fuel Consumtion at Cruise (1/h)	0,600	0,00016667	(1/s)			Refer to conversion details in the above text.
2	Specific Fuel Consumtion at Loiter (1/h)	0,720	0,00020000	(1/s)			Refer to conversion details in the above text.
3	Required Range (Km)	3 500,00	3 500 000	(m)			Convert Range to meters.
4	Cruise Speed (Mach)	0,53	174,35	(m/s)	649,50	(Km/h)	Conversion to m/s and Km/h.
5	Loiter Time (Min)	60,000	3 600,00	(s)			Conversion from hours to Seconds.
		Mission Segments Weights Fractions					
1	Empty Weight Fraction - Coefficient A	0,96					Table 3, Twin TurboProp.
2	Empty Weight Fraction - Coefficient C	-0,05					Table 3, Twin TurboProp.
3	Empty Weight Fraction - Coefficient K	1,00					Table 3, Fixed sweep wing.
4	Fuel Fraction - Warmup and Takeoff	0,970					Table 4.
5	Fuel Fraction - Climb	0,985					Table 4.
6	Fuel Fraction - Prop. Cruise Segment	0,791					Equation (13).
7	Fuel Fraction - Prop. Loiter Segment	0,944					Equation (14).
8	Fuel Fraction - Landing	0,995					Table 4.
9	Total Fuel Fraction with 6 % allowance - Propeller	0,308					Equation (19) and (20)
		Mission Segments Weights					
1	Aircraft Takeoff Weight (Kg)	128 645,1					Iterative solving of Equation (12)
2	Aircraft Empty Weight (Kg)	68 579,6					Table (3) using Takeoff Weight and Coefficients above.
3	Crew Weight (Kg)	500,0					05 crew members, with 100 Kg each , this makes it 500 Kg.
4	Payload Weight (Kg)	20 000,0					From design requirements.
5	Total Fuel Weight (Kg)	39 565,5					Iterative solving of Equation (12), then use weight fraction above.
6	Aircraft Weight - End of Warmup and Takeoff (Kg)	124 785,8					Weight at the end of the Warmup and Takeoff segment.
7	Aircraft Weight - End of Climb (Kg)	122 914,0					Weight at the end of the Climb segment.
8	Aircraft Weight - End of Prop. Cruise Segment (Kg)	97 272,2					Weight at the end of the Cruise Segment segment.
9	Aircraft Weight - End of Prop. Loiter Segment (Kg)	91 778,0					Weight at the end of the Loiter Segment segment.
10	Aircraft Weight - End of Landing (Kg)	91 319,2					Weight at the end of the Landing segment.
11	Reserves and Trapped Fuel - 6 % Allowance (Kg)	6 098,9					Weight of the 6 % fuel allowance.
12	Average Cruising Weight (Kg)	109 344,0					Equation (47), using End of Climb and End of Cruise Weights.
		Wing Parameters					
1	Takeoff Wing Loading Index	6,413					Figure 5, Value of wing loading is seletced between 6 and 7.
2	Takeoff Wing Loading (Kg/m2)	450,1					Equation (8).
3	Wing Leading Edge Sweep Angle (deg)	4,9	0,0847	(rad)			Equation (9), using method described in Point 4.4.
4	Wing Area (m2)	285,80					Equation (22).
5	Wing Span (m)	54,26					Equation (2).
6	Taper Ratio	0,40					Equation (10), using method described in Point 4.4.
7	Root Chord (m)	7,51					Equation (4).
8	Tip Chord (m)	3,02					Equation (3).
9	Quarter Chord Sweep (deg)	2,50	0,0436	(rad)			Equation (10), using method described in Point 4.4.
10	Mean Chord Length (m)	5,6					Equation (6).
11	AC Distance from Fuselage (m)	11,6					Equation (7).
12	AC Distance from Leading Edge (m)	1,4					Descriptive Text in Point 2.
13	Total Wetted Area(m2)	1 720,55					Description in Point 4.5.3.
14	Wing Zero Lift Angle (deg)	-1,25					Point 4.13.
15	Wing Incidence Angle (deg)	7,69					Equation (51).
		Aircraft Main Speeds					
1	Approach Speed (Knots)	130,0	66,88	(m/sec)	240,76	(Km/h)	Conversion to m/s and Km/h.
2	Min. Approach to Stall Coefficient	1,2					Table 12
3	Stall Speed (Knots)	108,3	55,7	(m/sec)	200,63	(Km/h)	Conversion to m/s and Km/h.
4	Cruise Altitude (m)	12 900,0					Conversion to m.
5	Air Density at Cruise Altitude (Kg/m3)	0,2697					Equation (46).
6	Air Density at Sea Level (Kg/m3)	1,2250					Equation (46) at zero meters.
		Lift Coefficients					
1	Maximum Lift Coefficient	2,32					Equation (41).
2	HLD Lift Coefficient Increment ΔCL	1,20					Table 14, Single slotted flap (1.2).
3	Maximum Clean Lift Coefficient CLmax	1,12					Equation (42).
4	Cruise lift Coefficient	0,92					Equation (45).
5	Lift Slop Coefficient CLα (1/rad)	5,87	0,1024	(1/deg)			Equation (24).

Table 17: Military Strategic Turboprop Airlifter Design Summary (Cont'd)

Nº	Parameter	Values and Units				Reference or Comment
		Calculated Aircraft Aerodynamic Features				
1	Oswald efficiency Factor ε	0,808				Equation (25).
2	Drag-due-to-Lift factor K	0,038				Equation (26).
3	CDo at Max(L/D)	0,0234				Equation (34), solved for CD_0.
4	Cruise Drag Coefficient	0,047				Equation (35).
5	Loiter Lift Coefficient	1,36				Equation (37).
6	Loiter Drag Coefficient	0,094				Equation (38).
7	Lift-to-drag ratio at Cruise	16,70				Computed lift-to-drag ratio at cruise using Equation (33).
8	Lift-to-drag ratio at Loiter	14,46				Computed lift-to-drag ratio at Loiter using Equation (36).
9	Cfe Subsonic	0,0053				Equation (23).
		Airfoil Calculated Features				
1	Effective Mach Number (Mach)	0,53				Equation (40).
2	Aerodynamic Sophistication Figure Factor M*	1,00				Conventional airfoils.
3	Wing airfoil thickness t/c	0,323	32,3%	(%)		Equation (39).
4	Airfoil Ideal Lift Coefficient Cli	0,70				Equation (48).
5	Airfoil Maximum Lift Ceofficient Clmax	1,32				Equation (43).
6	Airfoil lift curve slope C_l_alpha	7,115	0,1024	(1/deg)		Equation (49).

Based on the resulting parameters, Figure 23 provides an overview on the obtained aircraft weights allotment.
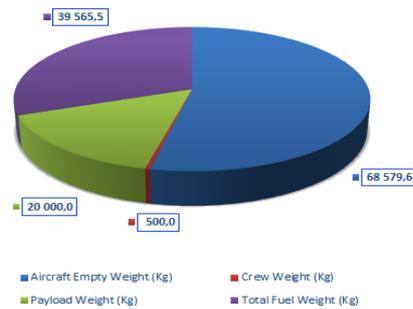

Figure 23: Obtained Weight Allotment – Turboprop Airlifter

Simulation Using OpenVSP:

Figure 24 illustrates the 3D-view of the obtained wing based on the wing parameters summarized in Table 17.
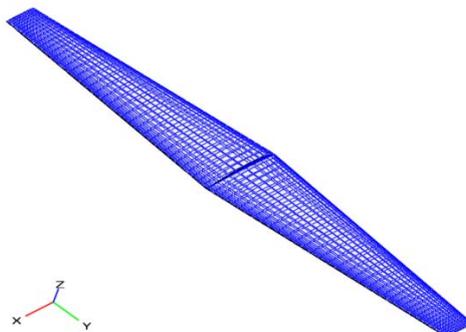

Figure 24: OpenVSP 3D-View of the Obtained Wing

Based on all the calculated airfoil features, the NACA 4424 illustrated in Figure 25 is selected for this design. The thickness of 32 % is much extravagant to meet the requirements.

Figure 25: Illustration of the NACA 4424

The OpenVSP Simulation corrected the wing incidence angle at cruise to 0.87 degrees. At this angle the wing pitching moment along the X-Axis is zero. Figure 26 illustrate the yielded wing lift coefficient distribution, it is a satisfactory practical elliptical distribution and reflects well the obtained Oswald efficiency factor of 0.808. A geometrical twist angle of -1.5 degrees has been applied to the wing, it is the best angle that yields zero lift coefficient at the tips of the wing.
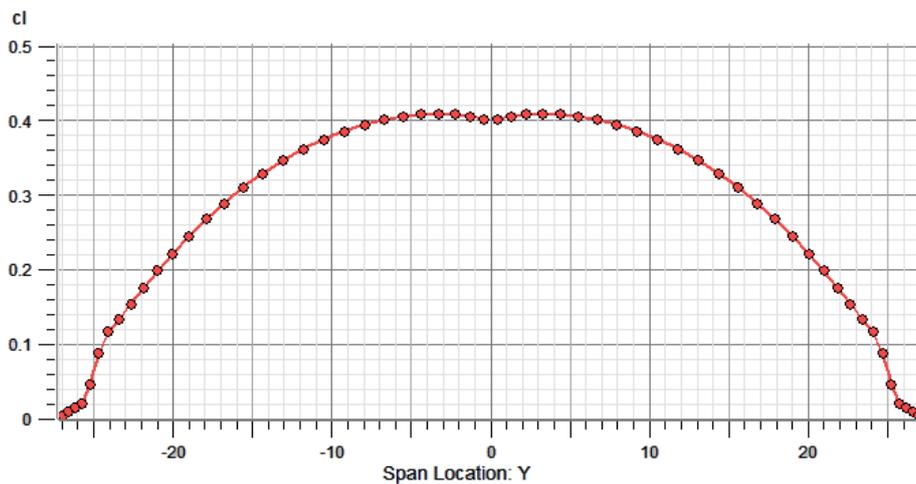

Figure 26: Wing Lift Coefficient Distribution

Figure 27 shows the mean-chord normalized load distribution. It is also an elliptical-like distribution.
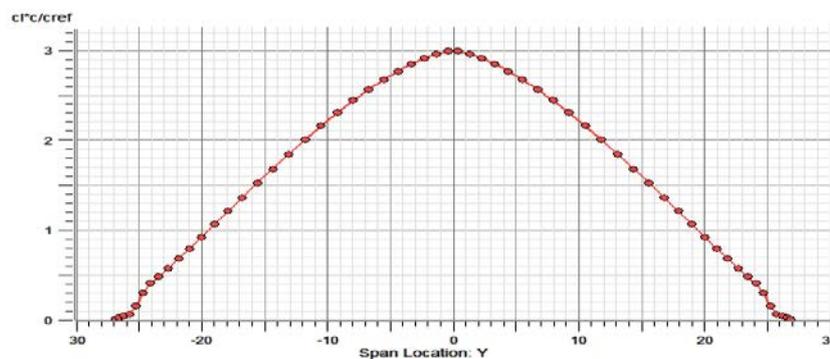

Figure 27: Normalized Wing Load Distribution

Figure 28 shows the obtained pressure coefficient difference (Delta-CP) spreading over the wing. The pressure coefficient difference indorses the obtained elliptical lift and load distributions.
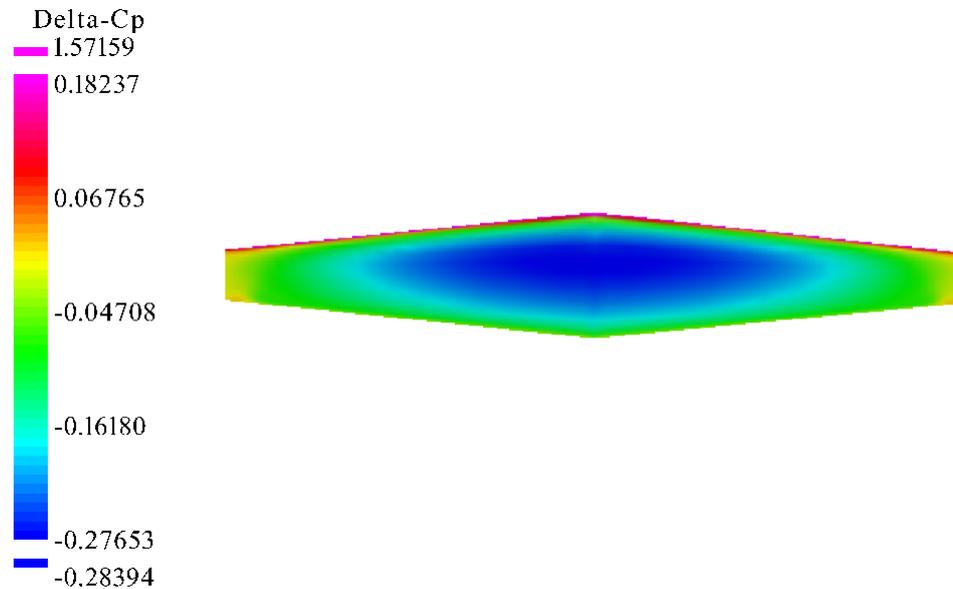

Figure 28: Pressure Coefficient Difference (Delta-CP) Distribution

The Challenge:

As stated in the flow chart (Figure 4), the above could be treated differently. Let's say for example that the efficiency of the turboprop engines decreases drastically at the cruise altitude of 12,900 m. However, the engines operates efficiently at 11,800 m. In this case, the aircraft must be designed to cruise at this altitude, the easiest thing to do, would be to play on the wing loading, the convergence is obtained for a wing loading of 689.6 $Kg/_{m^2}$ (loading index = 7.48).

This wing loading is too high for this class of aircraft (refer to Figure 5), it is expensive as well to build a wing to withstand such load. The way out from this problematic, would be to increase maximum lift to drag ratio (decrease the wet area ratio). Convergence has been achieved with the following parameters: aspect ratio = 10.3, wetted area ratio = 4.40, maximum lift to drag ratio = 16.72, wetted aspect ratio = 2.34 and the aircraft takeoff weight has been reduced to 128.645 Tons.

It is also important to note that from aerodynamic perspective, it is very challenging to design an aircraft of this class with such low wetted area ratio. This example reflects well the challenges related to the aircraft optimization process.

Due to the challenges related to the design of new aircrafts and the associated development budgets, several successful aircraft designs with good aerodynamic features underwent upgrade of avionics, onboard equipment, radars, weaponry, control systems, more powerful and efficient engines, use of composite materials to reduce the total aircraft weight. This strategy extended the service life of many aircrafts to decades, such as Tu-95 and

B-52.

7. Conclusion

Designing an efficient aircraft wing requires time and effort. This paper proposes an integrated approach aiming wing optimization at subsonic speeds up to Mach 0.85 that best yields elliptical lift and load distribution. The method is based on a targeted overall aircraft aerodynamic features, mainly the maximum lift-to-drag ratio and overall parasitic drag. It is a recursive process where the maximum lift-to-drag and wetted area ratios are first postulated. After that, aircraft wing parameters are computed based on either historical trends or best available expressions. The parasitic drag is then calculated using the wing lift coefficient expression at cruise condition, this allows the computation of the maximum lift-to-drag ratio. Convergence is achieved when the postulated and computed maximum lift-to-drag ratios are alike and the Equivalent Skin-Friction Coefficient reflects the aircraft class. Two aircraft layouts are designed and simulations are conducted using the NASA OpenVSP software, which confirmed the validity of the suggested approach.

Probing deeper, the proposed method and materials in this paper provide a strong foundation for future work in aircraft design in general and wing design specifically. One area of future work is in the enhancement of the efficiency of the technique by considering fuselage effect and winglets on lift, drag and pitching moment. Another area is the consideration of non-constant wing sweeps such as the highly swept inboard and Low sweep outboard wings or all variable sweep wings.

References

[1] Su-27 the Best Fighter in the World, Wings of Russia Studio.

[2] Raymer, D.P., "Aircraft Design: A Conceptual Approach", American Institute of Aeronautics and Astronautics, Washington D.C.

[3] M&AE 5070 - Dynamics of Flight Vehicles, Chapter 2: Aerodynamic Background.

[4] Prof. E.G. Tulapurkara, Airplane design (Aerodynamic), Chapter 5 Wing design - Selection of Wing Parameters – 3.

[5] National Aeronautics and Space Administration, Wing Design, Parts of an Airplane, Museum in the BOX Series.

[6] Mohammad Sadraey, Aircraft Design: A Systems Engineering Approach, Chapter 5: Wing Design.

[7] https://en.wikipedia.org/wiki/Kuznetsov_NK-32

[8] Shevell R. S., Fundamentals of Flight, Prentice Hall, Second edition, 1989.

[9] Howe, D.: Aircraft Conceptual Design Synthesis. London: Professional Engineering Publishing, 2000.

[10] USAF Test Pilot School Edwards AFB, CA, Volume I: Performance Phase, Chapter 11: Cruise Performance Theory.

[11] http://airfoiltools.com/search/index

[12] TORENBEEK, Egbert.: Synthesis of Subsonic Airplane Design. Delft: University Press, 1988.

[13] CIORNEI, Simona: Mach Number, Relative Thickness, Sweep And Lift Coefficient Of The Wing – An Empirical Investigation of Parameters and Equations. Hamburg University of Applied Sciences, Department of Automotive and Aeronautical Engineering, Project, 2005. – URL: http://Bibliothek.ProfScholz.de

[14] D. Scholz and S. Ciornei, Mach Number, Relative Thickness, Sweep and Lift Coefficient of the Wing – An Empirical Investigation of Parameters and Equations. Hamburg University of Applied Sciences Department of Automotive and Aeronautical Engineering Berliner Tor 9, 20099 Hamburg Germany.

[15] Shevell R. S., Fundamentals of Flight, Prentice Hall, Second edition, 1989.

[16] Greatrix, D.R., Powered Flight: The Engineering of Aerospace Propulsion, Chapter 2: Introduction to Atmospheric Flight, ISBN: 978-1-4471-2484-9.

[17] https://en.wikipedia.org/wiki/Pitching_moment

[18] http://www.aerospaceweb.org/question/airfoils/q0041.shtml

[19] http://www.openvsp.org/wiki/doku.php